Accepted Manuscript

Pyridinylimidazoles as dual glycogen synthase kinase 3β/p38α mitogen-activated protein kinase inhibitors

Fabian Heider, Francesco Ansideri, Roberta Tesch, Tatu Pantsar, Urs Haun, Eva Döring, Mark Kudolo, Antti Poso, Wolfgang Albrecht, Stefan A. Laufer, Pierre Koch

PII: S0223-5234(19)30350-2

DOI: https://doi.org/10.1016/j.ejmech.2019.04.035

Reference: EJMECH 11270

To appear in: *European Journal of Medicinal Chemistry*

Received Date: 27 January 2019

Revised Date: 29 March 2019

Accepted Date: 13 April 2019

Please cite this article as: F. Heider, F. Ansideri, R. Tesch, T. Pantsar, U. Haun, E. Döring, M. Kudolo, A. Poso, W. Albrecht, S.A. Laufer, P. Koch, Pyridinylimidazoles as dual glycogen synthase kinase 3β/p38α mitogen-activated protein kinase inhibitors, *European Journal of Medicinal Chemistry* (2019), doi: https://doi.org/10.1016/j.ejmech.2019.04.035.

Graphical Abstract

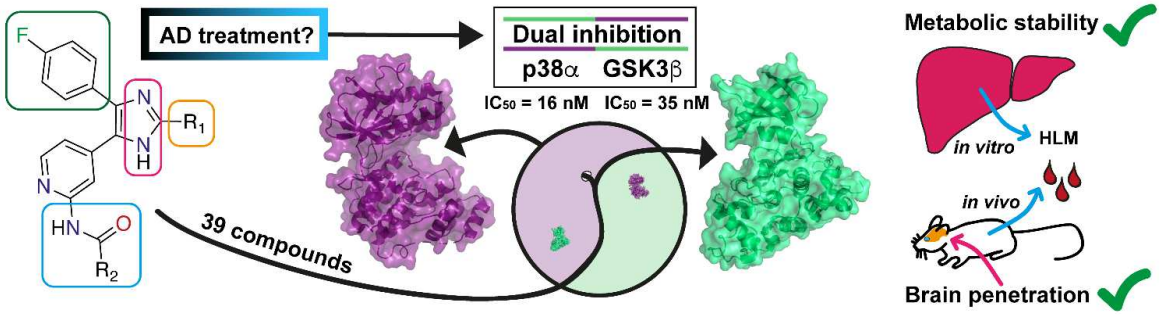

Pyridinylimidazoles as dual Glycogen Synthase Kinase 3β/p38α Mitogen-activated Protein Kinase Inhibitors

Fabian Heider,[1] Francesco Ansideri,[1] Roberta Tesch,[1] Tatu Pantsar,[2,3] Urs Haun,[1] Eva Döring,[1] Mark Kudolo,[1] Antti Poso,[2,3] Wolfgang Albrecht,[4] Stefan A. Laufer[1] and Pierre Koch[1,5]*

[1]Department of Pharmaceutical and Medicinal Chemistry, Institute of Pharmaceutical Sciences, Eberhard Karls Universität Tübingen, Auf der Morgenstelle 8, 72076 Tübingen, Germany

[2]School of Pharmacy, University of Eastern Finland, P.O.BOX 1627, 70211 Kuopio, Finland

[3]Department of Internal Medicine VIII, University Hospital Tübingen, Otfried-Müller-Strasse 14, 72076 Tübingen, Germany

[4]Teva-ratiopharm, Graf-Arco-Str. 3, 89079 Ulm, Germany

[5]Department of Pharmaceutical/Medicinal Chemistry II, Institute of Pharmacy, University of Regensburg, Universitätsstraße 31, 93053 Regensburg, Germany

*Corresponding author. Email address: pierre.koch@uni-tuebingen.de (P. Koch)

Abstract

Compounds simultaneously inhibiting two targets that are involved in the progression of the same complex disease may exhibit additive or even synergistic therapeutic effects. Here we unveil 2,4,5-trisubstituted imidazoles as dual inhibitors of p38α mitogen-activated protein kinase and glycogen synthase kinase 3β (GSK3β). Both enzymes are potential

therapeutic targets for neurodegenerative disorders, like Alzheimer's disease. A set of 39 compounds was synthesized and evaluated in kinase activity assays for their ability to inhibit both target kinases. Among the synthesized compounds, potent dual-target-directed inhibitors showing IC_{50} values down to the low double-digit nanomolar range, were identified. One of the best balanced dual inhibitors presented in here is *N*-(4-(2-ethyl-4-(4-fluorophenyl)-1*H*-imidazol-5-yl)pyridin-2-yl)cyclopropanecarboxamide (**20c**) (IC_{50} p38α: 16 nM; IC_{50} GSK3β: 35 nM) featuring an excellent metabolic stability and an appreciable isoform selectivity over the closely related GSK3α. Our findings were rationalized by computational docking studies based on previously published X-ray structures.

Keywords

Kinase inhibitors, pyridinylimidazoles, glycogen synthase kinase 3β, p38α MAP kinase, dual inhibitors, Alzheimer's disease.

1. Introduction

Neurodegenerative disorders, like Alzheimer's disease (AD), present one of the major medical challenges of the 21st century. It was estimated that in 2015 more than 46 million people worldwide were affected by AD.[1] With globally increasing life expectancy, the prevalence of AD is going to rise constantly. Currently, there are four active pharmaceutical ingredients approved by the FDA for the treatment of AD. However, none of them is able to stop or cure the disease. Therefore, there is a high unmet medical need for the development of new treatment options and strategies.

In the last decade, much effort has been put into the development of new therapeutic concepts – with little success. One of the reasons for the low clinical success rate of new therapies is undoubtedly the still poor understanding of the pathophysiology of AD. As AD

is a complex disease with a multicausal pathogenesis, a multi-target approach might be a promising and required strategy for the treatment of this devastating condition.

Several kinases have been implicated in the pathology of AD. Glycogen synthase kinase-3β (GSK3β) is a serine/threonine kinase for which significant evidence has been collected for its involvement in AD pathology over the years.[2-5] GSK3β is responsible for the hyperphosphorylation of the microtubule-associated protein tau, and is often referred to as a tau-kinase.[6, 7]' Overactivity of GSK3β has also been connected to an increased production of β-amyloids (Aβ),[8] memory deficits[9], oxidative stress and neuroinflammation.[10] Thus, the kinase plays a crucial role in almost every pathway leading to the hallmarks of AD.[11] The p38α mitogen-activated protein (MAP) kinase[12] is a serine/threonine kinase, which has been identified as a drug target for chronic inflammatory diseases since the mid-1990s.[13] This enzyme plays a central role in the biosynthesis of proinflammatory cytokines, like the tumor necrosis factor (TNF)-α, both at translational and transcriptional levels. The connection between the kinase and AD was drawn by Hensley *et al.*, who found increased activity of p38α MAP kinase in human postmortem brain tissue from AD patients.[14] Since then, an increasing amount of evidence has been piling up to establish a link between cytokine overproduction in the central nervous system (CNS) modulated by p38α MAP kinase and neuroinflammation.[15-18] Furthermore, the kinase has also been suspected to be involved in the hyperphosphorylation of tau proteins. A study with a brain-penetrant, selective p38α inhibitor significantly diminished tau phosphorylation and signs of insoluble tau aggregates on top of the expected reduction of proinflammatory cytokine released in a tauopathy mouse model.[19] Recently, two phase II studies on the selective p38α MAP kinase inhibitor Neflamapimod for the treatment of AD were completed successfully.[20, 21] Two follow-up phase II studies were launched in early 2018 (NCT03435861 & NCT03402659).

GSK3β and p38α MAP kinase both belong to the CMGC group and share an overall sequence similarity of 42 %. A closer analysis of their ATP binding pockets reveals several distinctions between the two enzymes (Figure 1). Most importantly the gatekeeper residue in p38α MAP kinase is Thr106, whereas a slightly bulkier Leu132 occupies this position in GSK3β. Moreover, the hinge region is composed of fairly different amino acids.

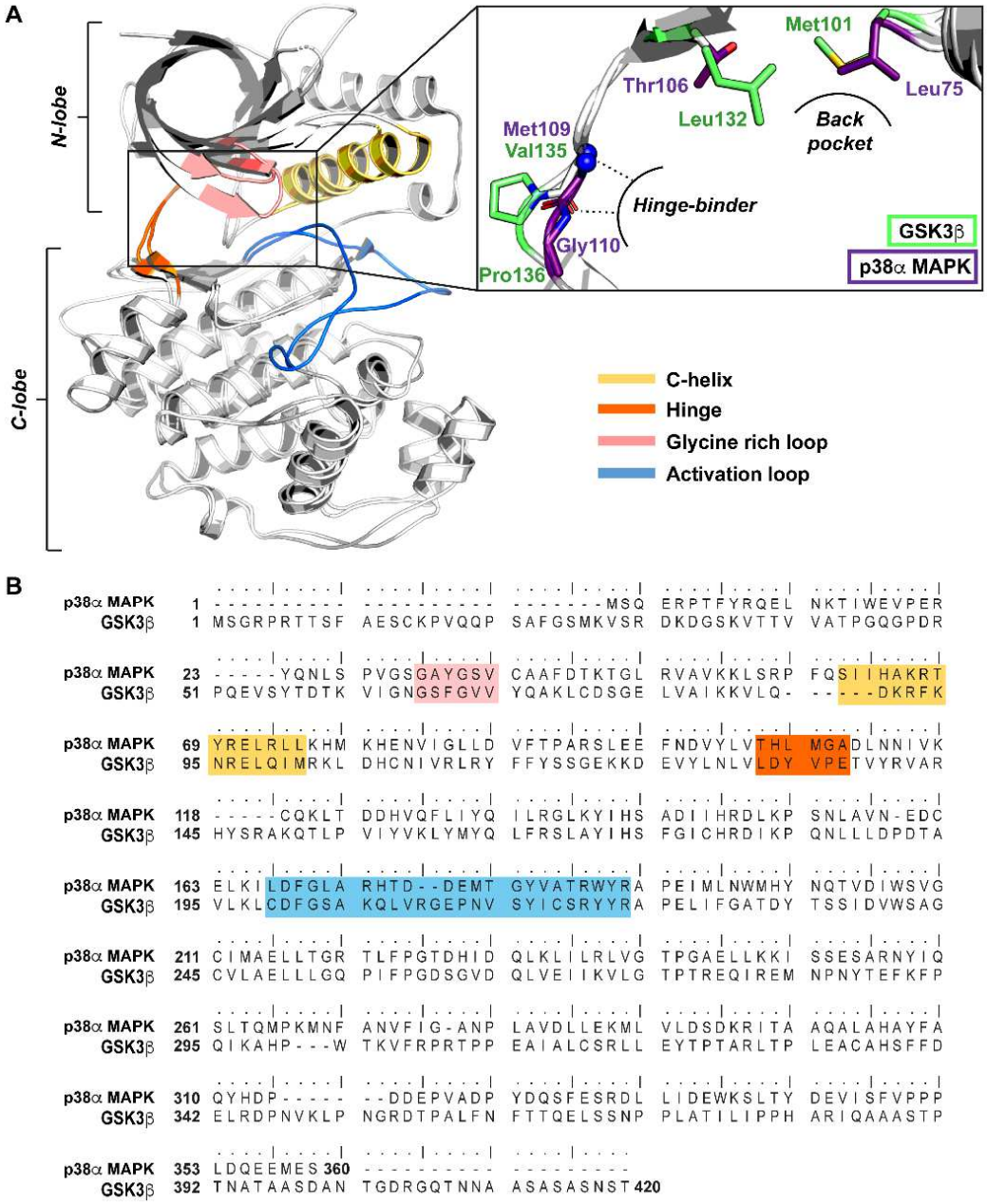

Figure 1. (A) Structural overlay of GSK3β and p38α MAP kinase. The most crucial differences in the amino acids of the ATP binding site are highlighted in green (GSK3β)

and purple (p38α MAP kinase). (B) Sequence alignment of GSK3β (UniProt code P49841) and p38α MAP kinase (UniProt code Q16539). The amino acids belonging to each region are highlighted as depicted in (A).

Pyridinylimidazoles are versatile scaffolds in kinase drug discovery and have been used to target several kinases such as p38α MAP kinase,[22-26] CK1δ,[27] TEK,[28] (triple mutant) EGFR[20] and the JNK family.[29, 30] Recently, synthetic strategies towards 2-alkylsulfanyl-4-aryl-5-(pyridin-4-yl)imidazoles as well as their biological activities were reviewed by our group.[31]

A screening of pyridinylimidazole-type p38α MAP kinase inhibitors from our in-house library (TüKIC, Tübingen Kinase Inhibitor Collection) versus GSK3β led to the identification of compound **1a**, serving as a lead compound for this study to design potent dual GSK3β/p38α MAP kinase inhibitors. Independently from us, compound **1a** has recently been disclosed by Halekotte *et al.* in an effort to synthesize CK1δ inhibitors.[27]

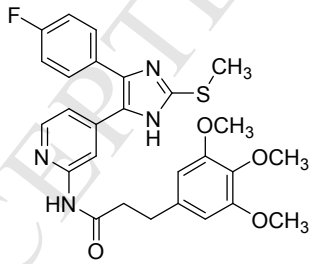

1a

IC_{50} (p38α) = 88 nM
IC_{50} (GSK3β) = 363 nM

Figure 2. Structure and biological data of in-house library screening hit **1a**.

Based on the initial screening data, first structure-activity relationships (SARs) were generated. An amide at the pyridine-C2 position seemed to be crucial for GSK3β activity. It was also assumed that 2,4,5-trisubstituted imidazoles, in general, show a higher affinity towards GSK3β than 1,2,4,5-tetrasubstituted imidazole derivatives. Previous SAR studies

on the p38α MAP kinase revealed that a tri- and tetrasubstitution pattern on the central imidazole core as well as a wide variety of substituents at the pyridine-C2 position (including amides) are well tolerated by the kinase.[31]

The aim of the present study was to design brain penetrant and metabolically stable dual inhibitors of GSK3β and p38α MAP kinase, which might serve as potential drugs for the treatment of neurodegenerative diseases. A series of 39 pyridinylimidazoles was synthesized and variations at the pyridine-C2 position, the imidazole-C2 and C4 positions as well as on both imidazole-N atoms were performed to further improve the GSK3β inhibitory activity while maintaining the excellent potency on p38α MAP kinase.

2. Results and Discussion

2.1. Chemistry

The 2-methylsulfanylimidazoles **1a**-**u** and 2-benzylsulfanylimidazoles **2a**-**e** were synthesized by a linear approach. Diversity at the pyridine-C2 position was introduced in the last step of the synthetic sequences (Schemes 1 and 2). The key intermediates 5-(2-aminopyridin-4-yl)imidazoles (**10a**, **10b**) were synthesized by a novel synthetic approach derived from a strategy published by our group in 2008 (Scheme 1).[24] Starting from *N*-Boc protected 2-amino-4-methylpyridine **3**, a *p*-methoxybenzyl (pMB) moiety was introduced as second protecting group of the amino function. The fully protected 4-picoline **4** was reacted with sodium hexamethyldisilazide (NaHMDS) in THF and ethyl 4-fluorobenzoate to obtain ethanone **5**. An excess of sodium nitrite dissolved in water was added dropwise to an acidic solution of **5** to give α-oximino ketone **6**. Subsequent treatment with Pd/C using hydrogen at atmospheric pressure in methanolic HCl resulted in both, reduction of the oximino group into a primary amino group as well as cleavage of the Boc group. Conveniently, the acid labile pMB was stable under these conditions. Cyclization of aminoketone **7** with potassium thiocyanate followed by the reaction with

methyl iodide or benzyl bromide resulted in *S*-substituted intermediates **9a** and **9b**, respectively. Finally, the pMB group was removed in neat trifluoroacetic acid (TFA) with gentle heating to yield the key intermediates **10a** and **10b**.

Scheme 1. Synthesis of key intermediates **10a** and **10b**.[a]

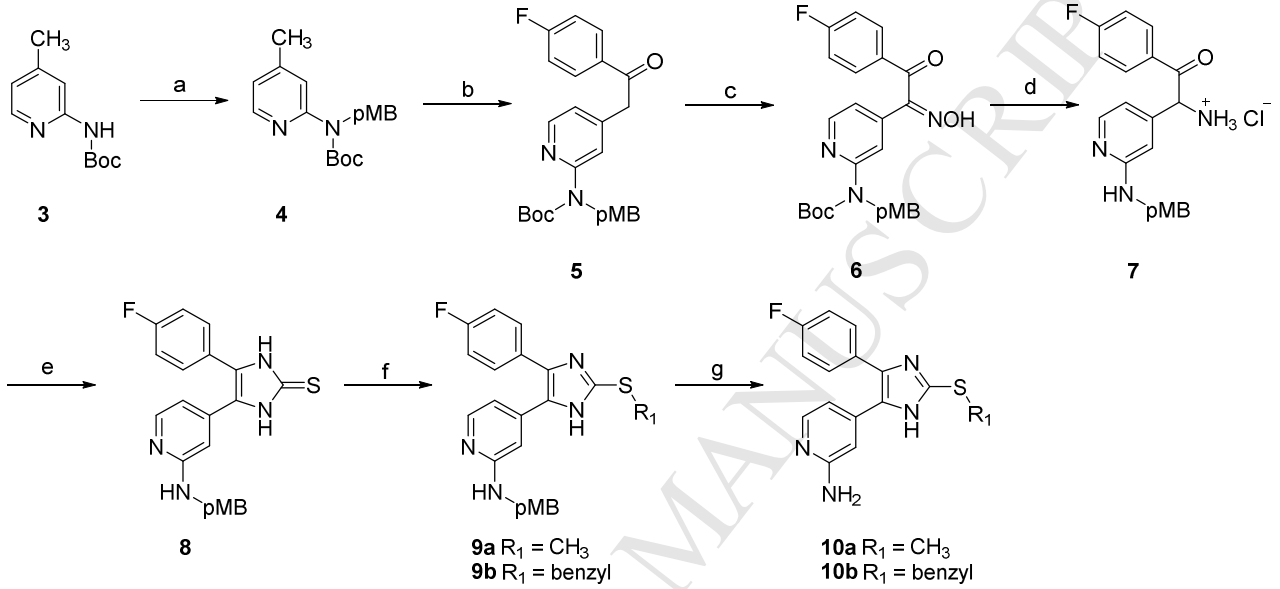

[a]Reagents and conditions: (a) NaH, 4-methoxybenzyl chloride, DMF, 0 °C then rt, 18 h; (b) NaHMDS, ethyl 4-fluorobenzoate, THF, 0 °C then rt, 2 h, 67% (over 2 steps); (c) $NaNO_2$, acetic acid, rt, 1 h, 100%; (d) H_2, Pd/C 10 %, methanolic HCl, 45 °C, 6 h; (e) KSCN, DMF, 160 °C, 2 h, 62% (over 2 steps); (f) CH_3I, NaO*t*Bu, MeOH, 55 °C, 2 h, 84% (in case of preparation of **11a**) or benzyl bromide, Cs_2CO_3, DMF, rt, 36 h, 35% (in case of preparation of **11b**); (g) TFA, 45 °C, 96-97%.

The acylamino function at the pyridine-C2 position of imidazoles **1b**, **1c**, **1s**, **2b,** and **2c** was introduced via Buchwald-Hartwig arylamidation by reacting known 2-chloropyridine derivatives **11a**-**b**[26, 32] with the corresponding amides in the presence of a Pd catalyst (Scheme 2). In case of imidazoles **1a**,**d**-**r**,**t**-**u** and **2a**,**d**-**e**, the amide moiety was installed the amide moiety was installed depending on the commercial availability of the starting

material either by direct acylation of 2-aminopridine derivates **10a** and **10b** with acid chlorides or by reacting **10a** and **10b** with the corresponding carboxylic acids in the presence of a coupling reagents. The sulfoxides **12a** and **12b** were obtained by oxidation of 2-methylsulfanylimidazoles **1c** and **1m** with hydrogen peroxide respectively. (Scheme 2).

Scheme 2. Synthesis of compounds **1a**-**u**, **2a**-**e** and sulfoxides **12a**-**b**.[a]

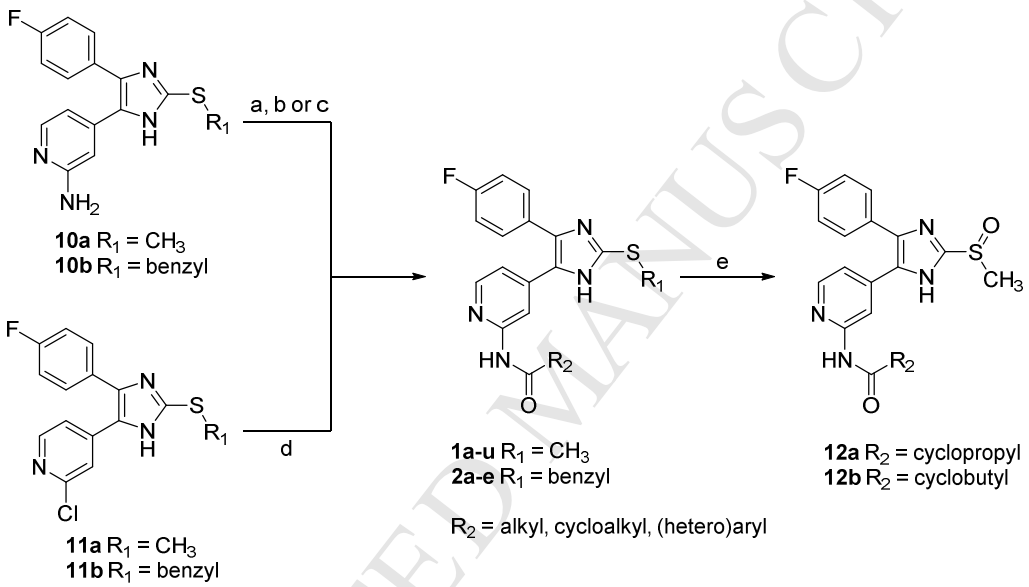

[a]Reagents and conditions: (a) carboxylic acid, PyBOP, DIPEA, DCM, rt, 40-93%; (b) carboxylic acid, HATU, DIPEA, DCM, rt, 21-85%; (c) acyl chloride, pyridine, 0 °C then rt; (d) amide, $Pd_2(dba)_3$, XantPhos, Cs_2CO_3, DMF, 100 °C, 16 h, 19-78%; (e) H_2O_2, MeCN, rt, 72-96 h, 42-51%. For R_2, see Tables 1-2.

The synthesis of tetrasubstituted imidazoles **14** and **16** started from known 4-(4-(4-fluorophenyl)-1-methyl-2-(methylthio)-1*H*-imidazol-5-yl)pyridin-2-amine **13**[25] and 2-chloro-4-(5-(4-fluorophenyl)-1-methyl-2-(methylthio)-1*H*-imidazol-4-yl)pyridine **15**,[22] respectively (Scheme 3). The cyclopropylamide moiety at the pyridine-C2 position was introduced either by reaction of pyridine-2-amine compound **13** and cyclopropanecarbonyl

chloride and the or by Buchwald-Hartwig arylamidation of 2-chloropyridine derivative **15** and cyclopropanecarboxamide.

Scheme 3. Synthesis of tetrasubstituted 2-acylaminopyridinylimidazole[a]

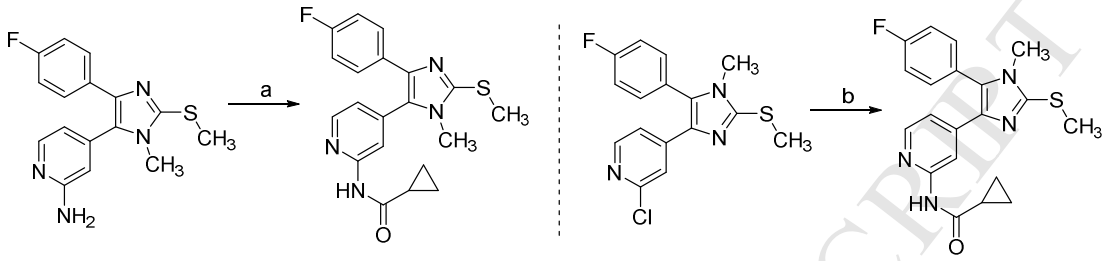

13 **14** **15** **16**

[a]Reagents and conditions: (a) cyclopropanecarbonyl chloride, pyridine, 0 °C then rt, 2 h, 31%; (b) cyclopropanecarboxamide, $Pd_2(dba)_3$, XantPhos, Cs_2CO_3, DMF, 100 °C, 16 h, 63%.

4,5-Disubstituted imidazole **20a** and 2,4,5-trisubstituted imidazoles **20b**-**g** were prepared in analogy to our recently reported protocol[33] based on the Radziszewski imidazole synthesis in four steps starting from ethanone **5** (Scheme 4). Treatment of **5** under Riley-Oxidation conditions yielded the corresponding α-diketone **17**. Under these acidic conditions, the Boc protecting group was already cleaved and in the next step, the pMB protecting group was removed using neat TFA. Then, the primary aromatic amine **18** was acylated with cyclopropanecarbonyl chloride. Interestingly, even using only one equivalent of acyl chloride, beside the expected monoacylated main product **19a** a substantial amount of double acylation (compound **19b**) was observed. Since the monoacylated product **19a**, however, could not be isolated, we used cyclopropanecarbonyl chloride in excess and continued our synthetic sequence with the double-acylated intermediate **19b**. Ring closing reaction to the imidazoles **20a-g** was achieved by reacting the α-diketone **19b** with ammonium acetate and different (hetero)aromatic, aliphatic aldehydes as well as

formaldehyde. Conveniently, the second acyl was cleaved during this step. The yields in this reaction fluctuated between 5% and 65%. The reaction of non-enolizable aldehydes gave generally significantly higher yields than aldehydes with an enolizable system. In case of latter ones, an acid catalyzed aldol-reaction took place before the ring closing reaction. For these compounds, we observed a second relatively distinct spot on the TLC and the mass of this spot corresponded to a molecule formed by ring closing reaction with the aldol product.

Scheme 4. Synthesis of 4-aryl-5-heteroaryl-substituted imidazole **20a** and 2-alkyl/aryl-4-aryl-5-heteroaryl-substituted Imidazole **20b**-**g**.[a]

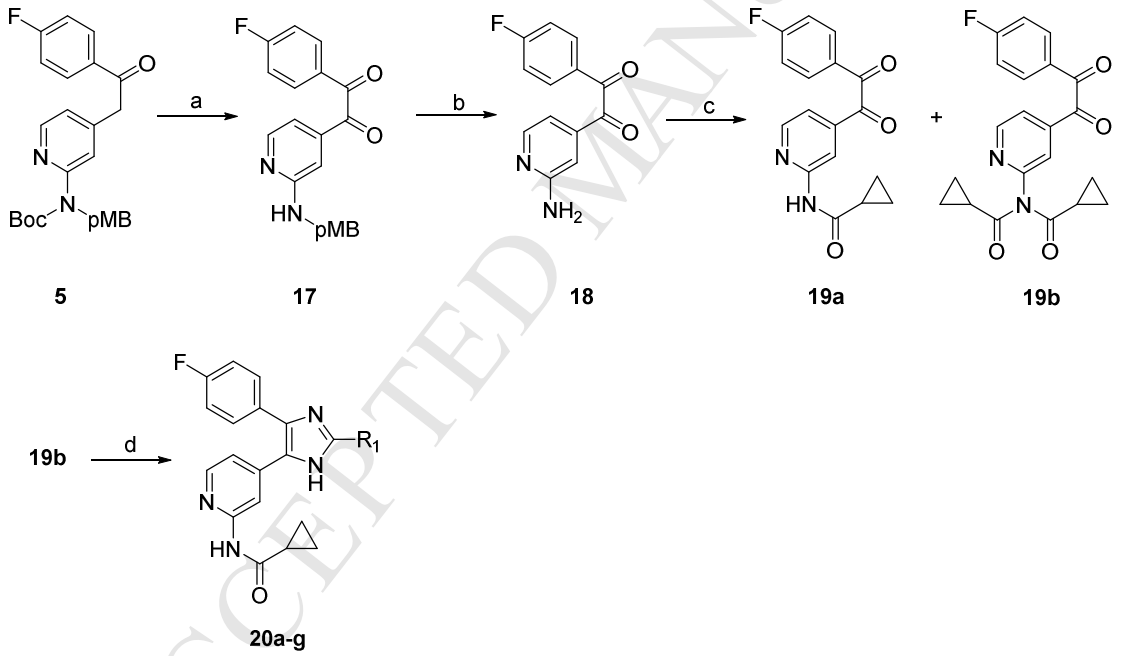

[a]Reagents and conditions: (a) SeO_2, acetic acid, 130 °C, 1.5 h, 44%; (b) TFA, rt, 97%; (c) cyclopropanecarbonyl chloride, DIPEA, DCM, rt, 18 h, 21%; (d) R_1-CHO, NH_4OAc, acetic acid, 130 °C, 3-4 h, 5-65%. For R_1, see Table 4.

The disubstituted imidazole **25** was prepared starting from commercially available 2-methylimidazole (**21**), which was protected in the first step using 2-(trimethylsilyl)ethoxymethyl (SEM) chloride (Scheme 5). A procedure previously described

by Markey and Kelly was used,[34] employing a directed *ortho*-metalation using *n*-butyllithium followed by the addition of tributyltin chloride, to obtain imidazole-5-stannane **23**. Intermediate **23** was reacted via a Stille coupling with *N*-(4-bromopyridin-2-yl)cyclopropanecarboxamide to yield imidazole **24**. Final product **25** was obtained after removal of the SEM protecting group under acidic conditions.

Scheme 5. Synthesis of 2-methyl-5-heteroaryl-substituted imidazole **25**.[a]

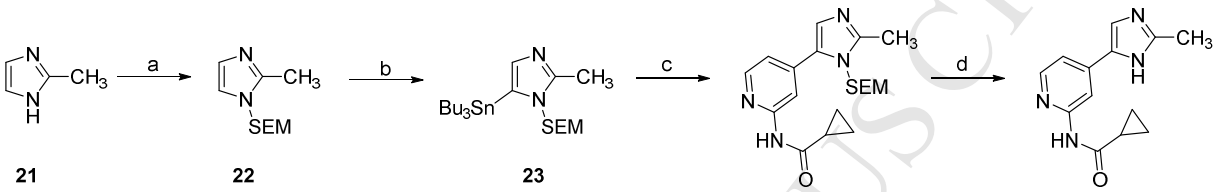

21 22 23 24 25

[a]Reagents and conditions: (a) NaH, 2-(trimethylsilyl)ethoxymethyl chloride, THF, 0 °C then rt, 18 h, 96%; (b) *n*-butyllithium, tributyltin chloride, Et_2O, 0 °C then rt, 2 h, 25%; (c) *N*-(4-bromopyridin-2-yl)cyclopropanecarboxamide, $Pd(PPh_3)_4$, 1,4-dioxane, 105 °C, 18 h, 77%; (d) TFA, DCM, rt, 6 h, 89%.

2.2. Biological Evaluation

2.2.1. Kinase activity assays and molecular modelling

The synthesized compounds were tested for their ability to inhibit p38α MAP kinase and GSK3β using an enzyme-linked immunosorbent assay (ELISA)[35] and the Promega ADP-Glo™ platform,[36] respectively. As reference compounds, we selected SB203580 (IC_{50} = 41 nM) for the p38α MAP kinase activity assay and SB216763 (IC_{50} = 89 nM) for the GSK3β assay. To estimate the GSK3 isoform selectivity, selected compounds were further evaluated for their inhibitory potency toward GSK3α using again the ADP-Glo™ activity assay. Specific inhibitors were further investigated for their metabolic stability in human liver microsomes (HLM) as well as in an *ex vivo* experiment for their ability to inhibit the

lipopolysaccharide (LPS)-stimulated TNF-α release from human whole blood (HWB).[37] In latter assay, SB203580 was used as reference compound (IC_{50} = 3,202 nM). Moreover, the two most promising inhibitors (**1c** and **20c**) were evaluated for their brain penetration, their cytochrome P450 (CYP450) inhibition as well as for their affinity to the human Ether-a-go-go-related gene (hERG) channel.

A possible binding mode for lead compound **1a** (Table 1) within the ATP binding site of p38α MAP kinase is depicted in Figure 3. The pyridine nitrogen atom as well as the NH at the pyridine-C2 position act as a classical donor-acceptor hinge-binding motif engaging in two H-bond interactions to the backbone of Met109 of the hinge region. A charge-assisted H-bond interaction occurs between the side chain of the Lys53 and the imidazole-N3 nitrogen. Moreover, the imidazole ring lays on top of the Phe169 forming an aromatic π–π stacking interaction. The 4-fluorophenyl ring occupies the hydrophobic region I (HR I). Access to this region is controlled by the gatekeeper residue Thr106. Targeting of HR I might be an important factor for selectivity over other protein kinases since bulkier gatekeepers often do not tolerate large substituents.[38]

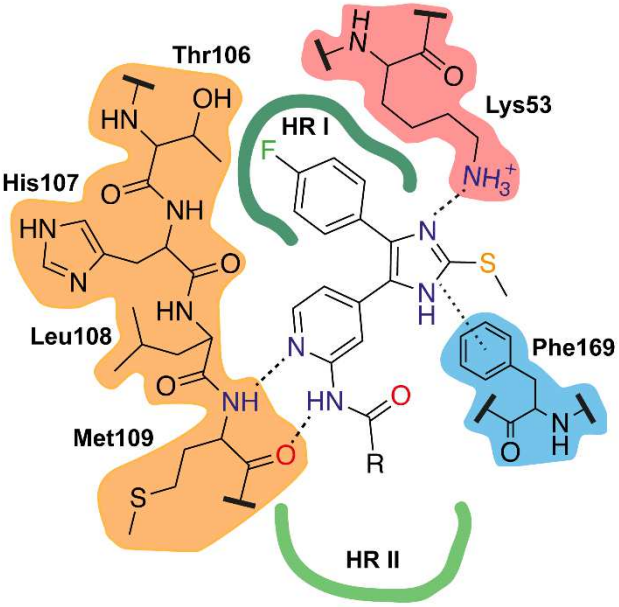

Figure 3. Two-dimensional schematic binding mode of pyridinylimidazoles in p38α MAP kinase. The binding mode is derived from published crystallographic data (PDB ID: 5ML5). The 4-fluorophenyl ring occupies HR I, while the HR II is rather large and solvent exposed. H-bonds and the π–π stacking interaction between the imidazole ring and Phe169 are indicated with a black dashed line.

Since different regions within the ATP binding site are highly conserved among all protein kinases, a similar binding mode of the lead compound **1a** was expected for GSK3β. Because of the gatekeeper on GSK3β being a bulkier amino acid (Leu132, in contrast to Thr106 in p38α MAP kinase), a simple rigid docking could lead to a misguided evaluation. Thus, we utilized an Induced Fit docking (IFD)[39-41] approach to study the binding to GSK3β. The IFD revealed a comparative binding mode of compound **1a** with GSK3β as in p38α MAP kinase. As depicted in Figure 4, the hinge-binding motif (pyridine-2-amine) is, as expected, able to act as a donor-acceptor to both, the carbonyl and NH group of Val135. Similar to the pose for p38α MAP kinase, the 4-fluorophenyl ring is located in the HR I of GSK3β. The proposed binding mode suggested a possible cation-π interaction between the 2,3,4-trimethoxyphenyl ring and Arg141. However, as the Lys85 in GSK3β is in a fixed conformation between two negatively charged residues, Asp200 and Glu97, and it is located farther away (compared to the corresponding Lys53 in p38α MAP kinase), we did not observe the charge-assisted H-bond between the imidazole ring and the Lys85. Instead, one of the imidazole tautomers is capable to form a H-bond with the Asp200 of the activation loop (part of the DFG motif). Since an equilibrium of the two possible tautomeric forms is expected, we suggest that the other imidazole tautomer (H-bond acceptor) may interact via a water-mediated H-bond with the Lys85. This interaction is observed in several X-ray structures of other protein kinases (e.g. JNK3) complexed with similar pyridinylimidazole-type inhibitors.[42]

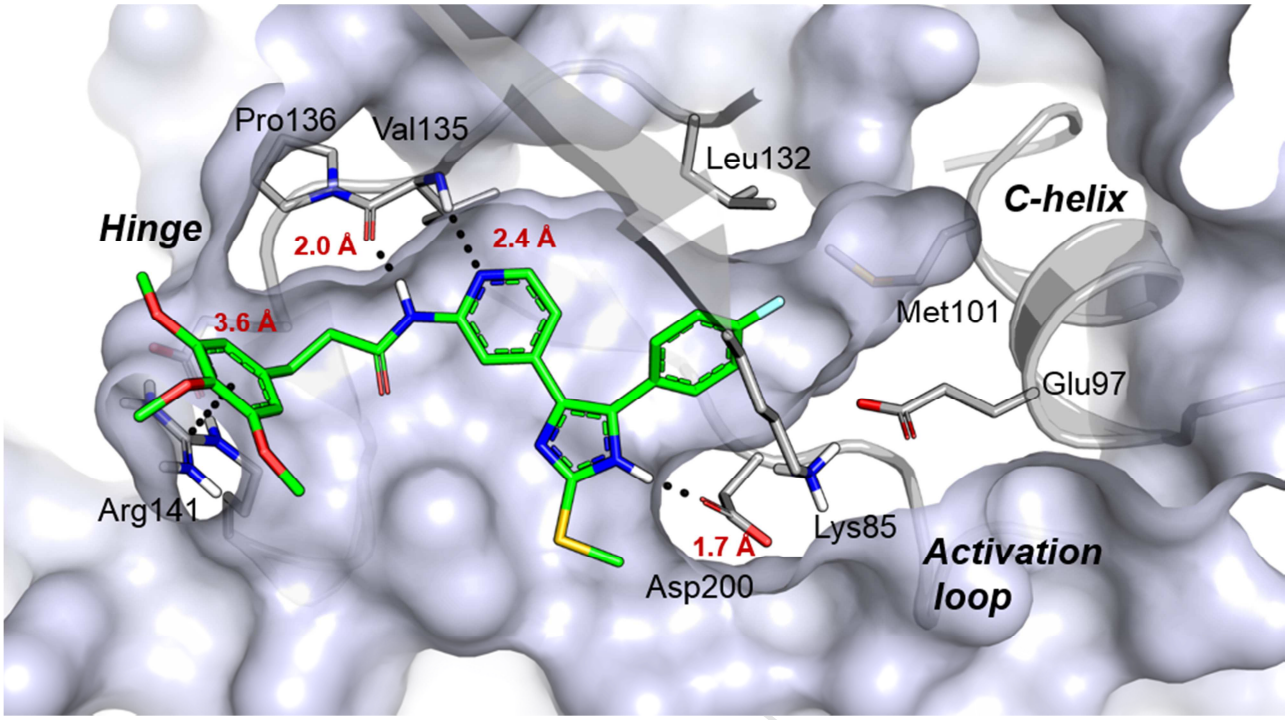

Figure 4. Proposed binding mode of **1a** on GSK3β obtained by IFD (PDB ID: 4PTC). H-bonds between the inhibitor and the kinase as well as the cation–π interaction between the trimethoxyphenyl ring and Arg141 are shown with black dashed lines.

Based on our initial HTS data analysis, we concluded that GSK3β inhibition was strongly enhanced when *N*-(pyridin-2-yl)amides instead of *N*-(pyridin-2-yl)amines were present at the pyridine-C2 position. From previous studies, we also knew that p38α MAP kinase tolerates both amines and amides in this position equally well.[25] Therefore, a set of compounds bearing different amides at the pyridine-C2 position was planned to collect first SAR, especially in regards to GSK3β. Our first synthetic efforts led to the series of compounds presented in Table 1 (**1b**-**u**).

Compared to the lead structure **1a**, the close analogs **1f** and **1g** bearing only one methoxy group at the phenyl ring are less active against GSK3β. This indicates that the electronic properties of the phenyl ring play an important role in the binding, probably, via contributing to the cation–π interaction with the Arg141 residue. The decreased electron

density in the phenyl ring could lead to a weakened cation–π interaction as electron-withdrawing substituents are known to attenuate these types of interactions. Consequently, inhibitor **1i** (GSK3β, IC_{50}: 995 nM) bearing an 3-(4-(trifluoromethyl)phenyl)propanamide moiety showed a 3-fold reduced GSK3β inhibition than the lead compound. These findings support our proposed orientation of our inhibitor molecule within the ATP bindings site. Meanwhile, these inhibitors (**1f**, **1g** and **1i)** retained their high inhibitory activity against p38α MAP kinase while displaying a substantial loss of activity versus GSK3β. Shortening of the C-linker of **1a** and **1i** by one methylene group resulted in compounds **1e** and **1h**, respectively. These compounds exhibited decreased GSK3β inhibition, while p38α MAP kinase inhibition of **1e** was increased almost by 7-fold compared to **1a**. To rationalize the data at hand, we decided to use already published crystal structures of p38α MAP kinase (PDB ID: 5ML5) and GSK3β (PDB ID: 4PTC) for the molecular modeling experiments. According to the computational approach, on GSK3β our compounds bind to the hinge region with two H-bonds to Val135, which is followed by Pro136, Glu137 and Thr138. Interestingly, Glu137 participates in a salt bridge interaction with Arg141 (Figure 5A). In the case of p38α MAP kinase, the corresponding amino acids are Met109, Gly110, Ala111 and Asp112, while the corresponding residue to the Arg141 on p38α MAP kinase is Asn115, which is unable to interact with the hinge region. Another important structural feature on p38α MAP kinase is the “glycine flip”. The peptide bond of Met109 and Gly110 can flip 180°, which has already been reported in the literature to explain the selectivity of another class of compounds.[43] Instead of the flexible glycine residue, GSK3β has a rigid Pro136 in this position. Finally, GSK3β has a bulky Tyr134 residue, which is stabilized on top of the hinge-region and forms a H-bond to the fixed Pro136 (Figure 5B). This Tyr134 occupies more space in the hinge region compared to the Leu108 in this position on p38α MAP kinase. Based on these three aspects, the flexibility of the residues in the hinge region, the stabilizing salt-bridge Glu137–Arg141 and the bulky

Tyr134, we hypothesize that the hinge region of GSK3β is clearly more constrained and crowded (in the vicinity of the hinge) than in p38α MAP kinase. This would explain the hindered binding of the shortened C-linker chain compounds **1e** and **1h** to GSK3β**.** The importance of these three aspects was further exemplified by the dramatical loss of activity towards GSK3β with the bulky and/or planar structural properties containing compounds **1j**, **1t** and **1u**.

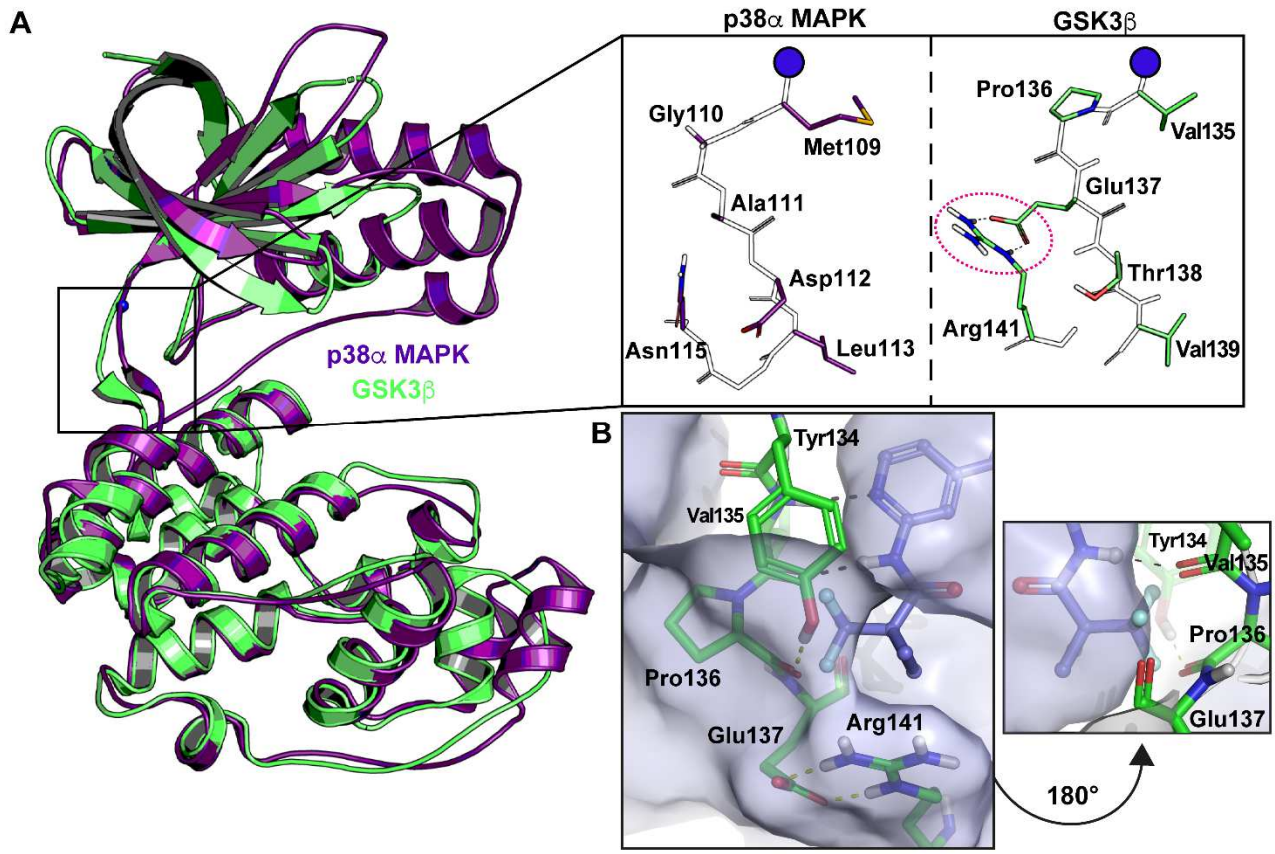

Figure 5. (A) Differences in the hinge region of p38α MAP kinase (purple) and GSK3β (green). The activation loops of both structures are omitted for clarity. The blue sphere represents the NH group of Met109 and Val135 in each kinase that forms a H-bond with the pyridine. The stabilizing salt bridge between Glu137 and Arg141 in GSK3β is highlighted by a red circle. **(B)** The rigid environment of the GSK3β hinge region prevents the accommodation of compounds with bulkier moieties in close proximity to the hinge binding motif. Compound **1j** is unable to fit into the GSK3β while maintaining H-bonding to

329 the hinge. The (trifluoromethyl)cyclopropyl moiety clash with the protein is illustrated here
330 by crossing the cavity surface (PDB ID: 4PTC).

331

332 **Table 1**. Structures and kinase activity of 2-methylsulfanylimidazoles **1a-u**, **14**, **16** and **37**.

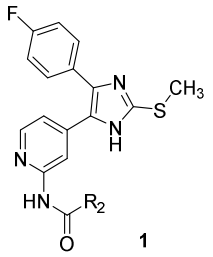

1

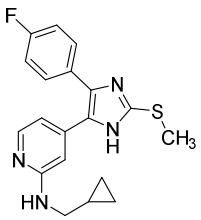

26

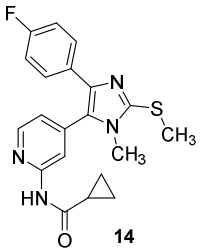

14

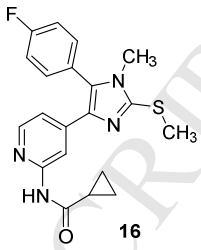

16

		IC_{50} [nM] ± SEM	
Cpd	**R_2**	**p38α MAP kinase**[a]	**GSK3β**[b]
1a	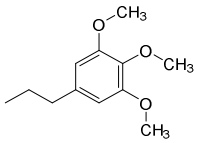	88 ± 8	363 ± 16
1b		45 ± 1	152 ± 9
1c		24 ± 0	40 ± 5
1d		40 ± 0.4	136 ± 45
1e	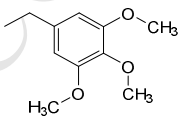	13 ± 1	510 ± 43
1f	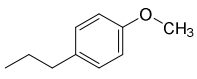	55 ± 6	542 ± 34
1g	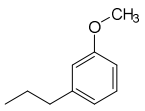	36 ± 2	471 ± 15

1h	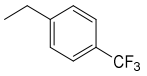	29 ± 1	3,242 ± 592
1i	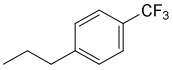	27 ± 2	956 ± 56
1j		184 ± 53	> 10,000
1k	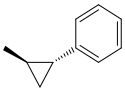	15 ± 0.1	808 ± 31
1l		15 ± 0	215 ± 49
1m		27 ± 0	132 ± 9
1n	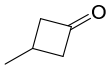	20 ± 1	183 ± 7
1o	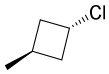	38 ± 0	395 ± 69
1p	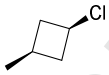	18 ± 0	170 ± 7
1q	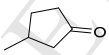	21 ± 1	73 ± 7
1r		28 ± 2	527 ± 44
1s	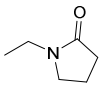	23 ± 0.4	126 ± 23
1t		22 ± 1	3,654 ± 115
1u		42 ± 8	> 10,000

26	--	14 ± 0	> 10,000
14	--	222 ± 4	638 ± 19
16	--	1,603 ± 733	1,780 ± 16

[a] n = 3; [b] n = 2

With a molecular weight of >500 Da, the inhibitors discussed so far are fairly heavy when considering the desired properties needed for CNS penetration.[44] Additionally, our insights from the IFD urged us to abandon any bulky residues that may clash with the rigid hinge region of GSK3β. Therefore, analogs of lead structure **1a** bearing smaller moieties at the pyridine-C2 position were synthesized. Compound **1b** with an *N*-acetyl moiety at the pyridine-C2 amino function displays improved GSK3β inhibition (GSK3β, IC_{50}: 152 nM) and a promising p38α MAP kinase/GSK3β inhibition ratio of 3.3. Following this observation, a series of inhibitors (**1b-d, 1j, 1l-u**) were synthesized bearing small cycloalkanecarboxamide moieties at the pyridine-C2 position. Introduction of a cyclopropanecarboxamide resulted in the potent and balanced dual inhibitor **1c**, showing IC_{50} values down to the low double-digit nanomolar range for both target kinases (p38α, IC_{50}: 24 nM; GSK3β, IC_{50}: 40 nM).

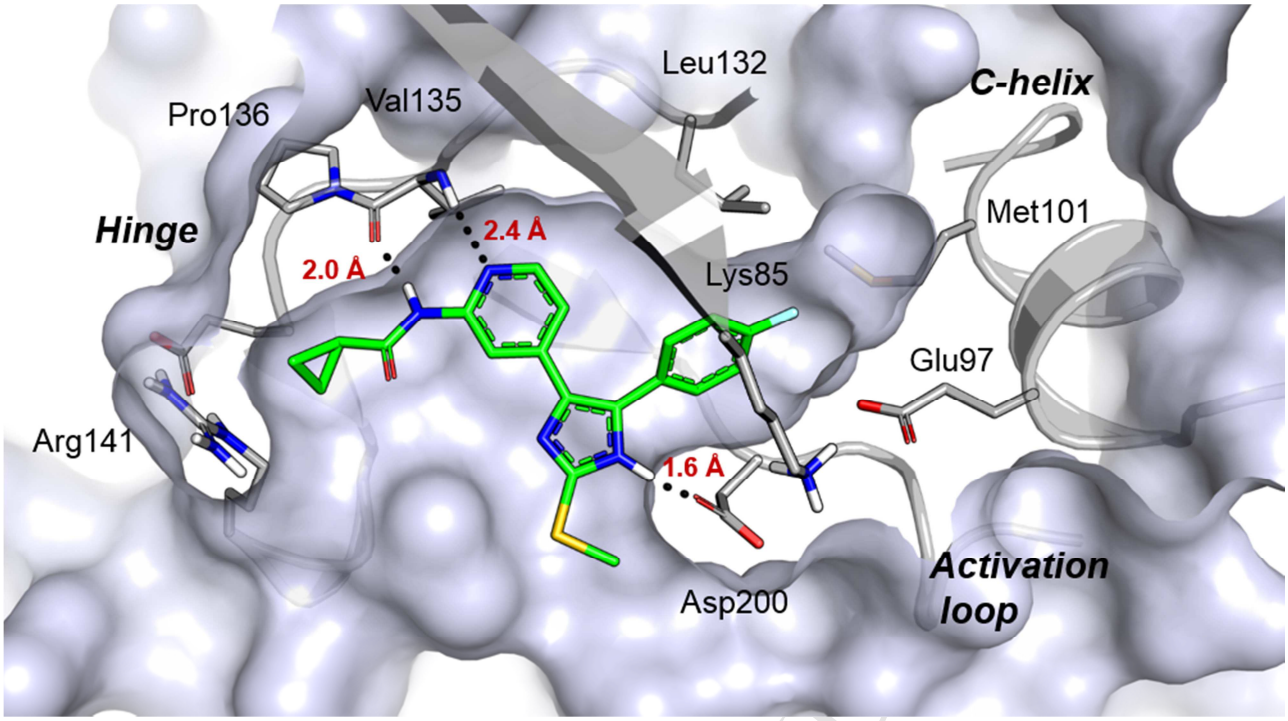

Figure 6. Proposed binding mode of **1c** on GSK3β obtained by IFD (PDB ID: 4PTC). The cyclopropyl moiety occupies ideally the small and rigid front pocket (HR II) area. H-bonds between the inhibitor and the kinase are shown as black dashed line.

Modifications on the cyclopropyl ring resulted in a loss of GSK3β activity. The introduction of a phenyl ring in position 2 of the cyclopropyl ring (**1k**) resulted in a slight improvement of p38α MAP kinase inhibition but also in a substantial drop of GSK3β activity. The change of the spacer length between the amide function and the cyclopropyl ring (**1l**) as well as replacement of the small cyclopropyl ring by bigger cyclobutyl (**1m**) or cyclopentyl (**1d**) rings decreased the GSK3β inhibitory potency slightly. The introduction of a trifluoromethyl group in position 1 of the cyclopropyl ring (**1j**) led to a complete loss of GSK3β activity, which is in good agreement with our hinge flexibility hypothesis (see Figure 5B). Interestingly, compound **1j** had also one order of magnitude reduced inhibitory potency on p38α MAP kinase, which indicates that the trifluoromethyl group attached to the cyclopropyl is already too close to the hinge region and may distort the H-bond interactions

with Met109 (see Figure 3). Nevertheless, the flexibility of the hinge region on p38α MAP kinase still enables the binding of this compound much better than GSK3β does.

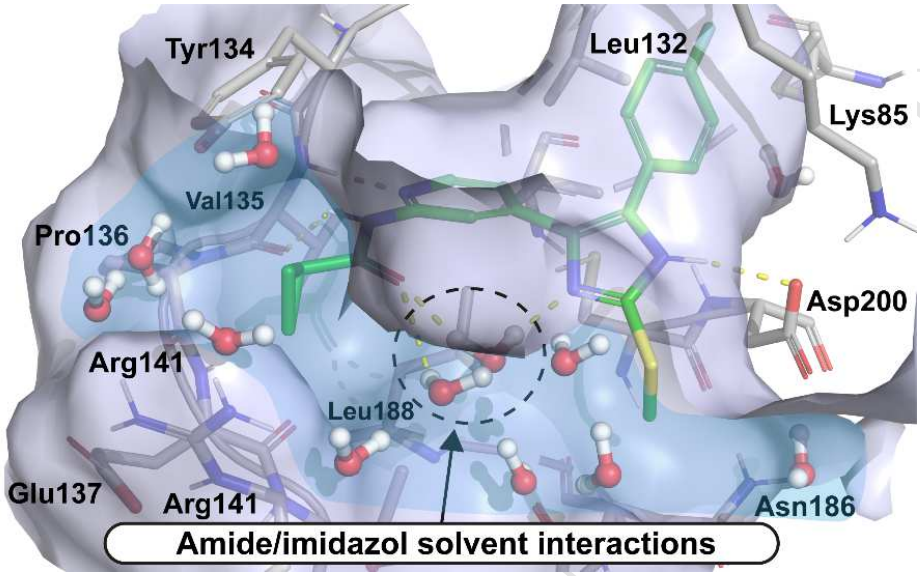

Figure 7. The output conformation of the compound **1c** after 200 ns MD simulation (PDB ID: 4PTC). The carbonyl group of the amide and the imidazole-N3 participate in the solvent interactions. The protein surface is illustrated with light purple color and the solvent access to the binding site is highlighted in blue. The water molecules are displayed within 4Å from the ligand.

Attempts to address the solvent interface (Figure 7) with more polar groups attached to small cycloalkyl groups in order to gain binding affinity through enthalpically favorable, stabilized water networks, resulted in compounds **1n** and **1q**. Compared to the cyclobutane analog **1m**, imidazole **1n** bearing a 3-oxocyclobutyl substituent at the amide function displayed no improvement in GSK3β inhibition. In comparison to the parent cyclopentyl compound **1d**, pyridinylimidazole **1q** having a 3-oxocyclopentyl substituent showed a 2-fold increased GSK3β inhibitory activity. The two *cis*/*trans* 3-chlorocyclobutyl isomers (**1o** and **1p**) showed a roughly 2-fold difference in inhibition for both kinases with the *cis*-isomer being the more potent one.

Compound **1s** bearing a 2-oxopyrrolidin-1-acetamide at the pyridine-C2 position displayed a similar p38α MAP kinase/GSK3β inhibition profile as **1d** bearing a cyclopentylamide at the same position. Imidazole **1r** having 2-tetrahydrofuranyl at the amide function showed a decreased GSK3β activity (factor 4) compared to **1d**. The introduction of aromatic heterocyclic rings directly at the amide function (**1t** and **1u**) resulted in a tremendous loss of GSK3β inhibitory activity as a consequence of the aforementioned rigidity of the GSK3β hinge region (Figure 5B). In contrast, none of the modifications at the pyridine-C2 position had any meaningful impact on p38α MAP kinase inhibition. All pyridinylimidazoles reported in Table 1 except **1j**, **14** and **16** are potent p38α MAP kinase inhibitors displaying IC_{50} values in the double-digit nanomolar range. Replacement of the carbonyl part of the amide group by a methylene group resulted in a complete loss of GSK3β affinity (compare **37** vs **1c**), whereas this modification slightly increased p38α MAP kinase inhibitory activity. Those findings exemplify the importance of the amide group at the pyridine-C2 for the binding to GSK3β. This arises most likely from solvent interactions that have been observed to play a crucial role for the compound affinity, as demonstrated in other studies.[45] Indeed, we noticed important solvent interactions with the amide in our molecular dynamics (MD) simulation (Figure 7). Moreover, there seems to be a possibility for solvent mediated, bridged interactions between the amide carbonyl and the imidazole-N3. This may help to stabilize the active conformation of the molecule, ultimately enhancing the overall binding affinity. Interestingly, this effect was only dramatic with GSK3β. The bulky and charged Arg141 residue in GSK3β clearly shields the solvent access to the binding site and influences to the water network organization. In case of the more flexible and open p38α MAP kinase, the water network reorganization within the pocket is tolerated thus enabling the binding of **37**.

The introduction of substituents on the imidazole-N1 or -N3 atom of potent dual p38α MAP kinase/GSK3β inhibitor **1c** resulted in a drop of both GSK3β and p38α MAP kinase

inhibitory activity (compounds **14** and **16**). This effect was more pronounced in the case of **16**. The methylation of the nitrogen atom adjacent to the 4-fluorophenyl ring resulted in two orders of magnitude reduced p38α MAP kinase inhibitory activity, compromising the charge-assisted H-bond to the Lys53 (see Figure 3). In addition, in the case of GSK3β, **16** would also disrupt either the H-bond to Asp200 or the potential water-mediated interaction to Lys85 depending on the NH tautomerism (see Figure 4).

In previous studies, our group showed that bigger moieties at the imidazole-C2 position were well tolerated by p38α MAP kinase.[24] Therefore, the inhibitory potency of a small series of 5 compounds, wherein the *S*-methyl group at this position was replaced by a *S*-benzyl group, was evaluated (Table 2). In case of GSK3β, imidazoles **2a-d** displayed a decreased affinity (3- to 6-fold) in comparison to their *S*-methyl counterparts **1a-d**

Table 2. Structures and kinase activity of 2-benzylsulfanylimidazole **2a-e**.

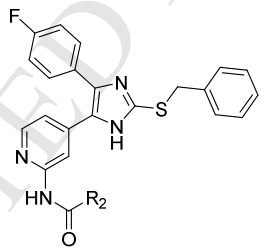

		IC_{50} [nM] ± SEM	
Cpd	**R_2**	**p38α MAP kinase**[a]	**GSK3β**[b]
2a	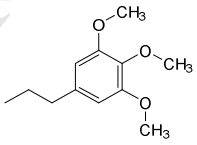	61 ± 4	1,149 ± 167
2b		51 ± 5	560 ± 23
2c		41 ± 3	229 ± 3

2d		20 ± 2	663 ± 45
2e	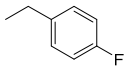	3 ± 0	1,499 ± 51

[a] n = 3; [b] n = 2

Computational studies of **2c** with GSK3β revealed that the *S*-benzyl substituent is oriented towards the solvent accessible region and displays contacts with the lipophilic glycine rich loop residues, mainly with Phe67, Val70, and Ile62. In agreement with previous observations, imidazoles **2a-e** bearing *S*-benzyl moiety at the imidazole-C2 position displayed similar p38α MAP kinase inhibitory activity as their *S*-methyl counterparts. Compound **2e** with a 4-fluorophenylacetamide at the pyridine-C2 position represents the most potent p38α MAP kinase inhibitor in this series having an IC_{50} value in the low single-digit nanomolar range and displaying a greater than 500-fold selectivity over GSK3β.

Previous studies on *in vitro* metabolic stability of similar p38α MAP kinase inhibitors revealed that the alkylsulfanyl moiety at the imidazole-C2 position is susceptible to oxidation, resulting in the corresponding 2-alkylsulfinylimidazoles as main metabolites.[33, 46] To estimate the impact of the metabolism on the inhibition profile, the corresponding sulfoxides of **1c** and **1m** were additionally evaluated for their ability to inhibit both target kinases (Table 3). Sulfoxides **12a** and **12b** showed a 3- and 6-fold reduced GSK3β inhibition compared to **1c** and **1m**, respectively, while the two compounds displayed a similar p38α MAP kinase inhibition profile like their *S*-methyl counterparts.

Table 3. Structures and kinase activity of 2-methylsulfinylimidazoles **12a** and **12b**.

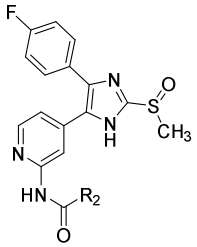

Cpd	R_1	R_2	IC_{50} [nM] ± SEM	
			p38α MAP kinase[a]	GSK3β[b]
12a			44 ± 0	236 ± 45
12b			29 ± 6	428 ± 19

[a] n = 3; [b] n = 2

In order to remove the metabolic hotspot of the 2-methylsulfanylimidazoles, another series of pyridinylimidazoles were synthesized wherein the imidazole-C2 position was modified. To this end, alkyl (**20b**,**c**), aryl (**20d**), arylalkyl (**20e**,**f**) and heteroaryl (**20g**) substituents were introduced to this position (Table 4). In case of p38α MAP kinase, substitution of the imidazole-C2 position had no influence on the inhibitory activity and compounds **20b**-**g** displayed IC_{50} values in the same range as the simple disubstituted imidazole **20a**. Looking at GSK3β, introduction of a phenyl residue (**20d**) led to a distinctly reduced inhibitory potency. Compared to **20a**, imidazole **20c** with a small ethyl moiety at the imidazole C2-position is the only example in this series displaying a significantly improved inhibition as well as a p38α MAP kinase/GSK3β inhibition profile similar to the most potent compound out of the *S*-methyl series (**1c**).

Table 4. Structures and kinase activity of 4,5-disubstitued imidazole **20a** and 2,4,5-trisubstitued imidazoles **20b**-**g**.

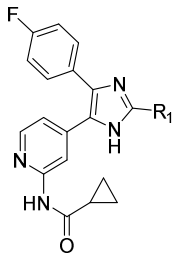

20a-g

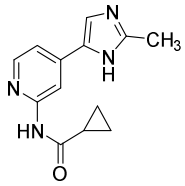

25

Cpd	R_1	IC_{50} [nM] ± SEM	
		p38α MAP kinase[a]	GSK3β[b]
20a		19 ± 1	64 ± 4
20b		19 ± 1	53 ± 12
20c		16 ± 1	35 ± 6
20d		27 ± 1	570 ± 98
20e	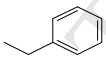	18 ± 0	59 ± 11
20f	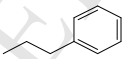	20 ± 0.5	133 ± 7
20g		18 ± 1	156 ± 14
25		>10,000 (1 %)[c]	1,684 ± 120

[a]n = 3; [b]n = 2; [c]percent inhibition at indicated concentration, tested in a LANCE assay at Eurofins Cerep SA, France (reference compound in this assay: SB203580, IC_{50} = 65 nM).

As observed in previous studies,[29, 42] the removal of the 4-fluorophenyl ring (**25**) led to a complete loss of p38α MAP kinase inhibitory activity (Table 5). Moreover, this structural modification resulted in a 32-fold reduced inhibitory activity of GSK3β (**25** vs. **20b**), demonstrating the importance of this residue also for GSK3β inhibition.

2.2.2. GSK3β ATP-competitiveness

Compounds **1c** and **20c** were tested at three different ATP concentrations (25 µM, 100 µM and 500 µM) to confirm their ATP-competitiveness. As we expected from our postulated binding mode, higher concentrations of ATP led to significantly increased IC_{50} values from 18 nM and 46 nM at 25 µM of ATP to 423 nM and 492 nM at 500 µM of ATP in case of **1c** and **20c**, respectively (Figures S3 and S4, supplementary data). This ATP-dependent behavior of both compounds is a strong indicator for ATP-competitive binding of this inhibitor class.

2.2.3. GSK3 isoform selectivity

The sequences of GSK3α and GSK3β are highly conserved, showing 98 % identity in the kinase domain.[47] The few existing variations in their amino acid composition are mostly minor changes and occur in areas that display no direct interactions with the ATP binding site. In the hinge region, the only difference is that the Asp133 of GSK3β is replaced by the Glu196 in GSK3α. The side-chain of Asp133/Glu196 is pointing outwards from the ATP pocket towards the solvent and is putatively interacting with the positively charged residues (*e.g.* Arg113 in GSK3β) in the solvent interface. To evaluate the structural influence of this difference among the isoforms is tedious as there is no publicly available crystal structures of GSK3α. During the preparation of this manuscript, however, Wagner and co-workers demonstrated that the switch between these two amino acids may have an influence on the topology of the ATP binding site and the HR I.[48] These changes in the

binding site dynamics might explain the slight selectivity of the selected 2-methylsulfanyl (**1a**,**c**), 2-benzylsulfanyl (**2c**) and 2-alkylimidazole (**20c**,**e**) derivatives for GSK3β versus GSK3α (Table 5). The closely related analogues **1c** and **20c** proved to be the most selective compounds with a 7.5- and 8.6-fold selectivity towards GSK3β, respectively.

Table 5. GSK3α/β isoform selectivity.

	IC_{50} [nM] ± SEM[a]	
Cpd	**GSK3β**	**GSK3α**
1c	40 ± 5	300 ± 31
2c	229 ± 3	853 ± 268
1a	363 ± 16	2,046 ± 220
12a	236 ± 45	1,337 ± 25
20c	35 ± 6	301 ± 22
20e	59 ± 11	428 ± 96

[a]n = 2

2.2.4. Metabolism

The two potent dual GSK3β/p38α MAP kinase inhibitors **1c** and **20c**, as well as the highly active and p38α MAP kinase selective compound **2e**, were further evaluated for their metabolic stability in mixed male&female HLM (Tables S1-S3, supplementary data). The

2-methylsulfanylimidazole **1c** was oxidized to the corresponding sulfoxide **12a** with a reasonable half-life of 190 min. After 4 h of incubation time, about 44 % of **1c** remained unmetabolized. Sulfoxide **12a** was detected as sole metabolite (65 % after 4 h). The cyclopropylamide moiety was not affected by the microsomes. In contrast, 2-ethlysulfanylimidazole **20c** showed excellent metabolic stability in the HLM experiment, leaving more than 90 % of the inhibitor unmetabolized after 4h. Benzylsulfanylimidazole **2e** exhibited better metabolic stability than **1c** although more metabolites were formed during the incubation (66 % of **2e** remained untouched after 4 h). Similar to the experiment with **1c**, the corresponding sulfoxide of **2e** was detected as the main metabolite (11 %). In addition, other biotransformation reactions took place on **2e** as well as on its sulfoxide, *e.g.* oxidation to the corresponding sulfone.

2.2.5. Pharmacokinetic and CNS penetration study

To further assess the plasma stability and evaluate brain penetration, the most potent dual p38α MAP kinase/GSK3β inhibitors **1c** and **20c** were tested in adult male RjOrl:Swiss CD-1 mice. The mice were treated with a single dose intravenous injection (10 mg/kg) and plasma samples were collected 10, 30 and 120 min after the dosing. After the last sample was obtained, the mice were sacrificed for dissection of the brains. Blood and brain samples were analyzed via LC-MS after preparation (see supplementary data).

In contrast to the *in vitro* HLM experiments, 2-methylsulfanylimidazole **1c** showed an even faster biotransformation rate to the corresponding sulfoxide **12a** *in vivo*. After 10 min, the ratio between *S*-methyl (**1c**) and sulfoxide (**12a**) was already 1:2. After 2 h, inhibitor **1c** was almost completely metabolized. The active metabolite **12a** showed a slight blood-brain barrier penetration (brain concentration: 65.8 ng/g after 2h), whereas the concentration of 2-methylsulfanylimidazole **1c** in the brain was one-order of magnitude lower. The *in vitro* metabolically stable inhibitor **20c** showed relatively fast plasma

clearance from 850 ng/mL after 10 min to 95 ng/mL after 2 h. The brain concentration of **20c** 2 h after dosing was 13.3 ng/g, which estimates a brain concentration of **20c** exceeding its IC_{50} values on GSK3β and p38α MAP kinase of 1.1-fold and 2.5-fold, respectively.

The HWB presents a possibility to evaluate the effectiveness of p38α MAP kinase inhibitors in regard to their modulation of proinflammatory cytokine secretion in a cell-based system represents the HWB assay.[37] In this *ex vivo* assay, the amount of TNF-α release from HWB after LPS-stimulation is quantified and the efficacy of the inhibitors is evaluated more specifically with respect to *in vivo* parameters like plasma protein binding and cellular permeability. The release of LPS-stimulated TNF-α from HWB was inhibited by the compounds **1c** and **20c** at concentrations in the submicromolar range (Table 6). In this assay, the 2-alkylimidazole derivative **20c** displayed slightly increased inhibition compared to the 2-methylsulfanyl derivative **1c**. This observation correlates well with the data from the p38α MAP kinase activity assay.

Table 6. Inhibition of LPS-stimulated TNF-α release from HWB as well as *in vitro* CYP and hERG Inhibition Data.

	IC_{50} [nM] ± SEM[a]	**% inhibition @ 10 μM**					
Cpd	**TNF-α release**	**hERG**	**CYP1A2**	**CYP2C9**	**CYP2C19**	**CYP2D6**	**CYP3A4**
1c	541 ± 217	30.1	88.4	77.7	56.1	14.6	75.6
20c	317 ± 4	43.3	83.6	83.6	81.7	58.3	75.1

[a]n = 2

Further pharmacological profiling of the dual p38α MAP kinase/GSK3β inhibitors **1c** and **20c** included the evaluation of their ability to inhibit hERG and relevant CYP isoforms (Table 6). At a test concentration of 10 µM, imidazole **1c** displays a 30 % inhibition of hERG and inhibits three of the tested CYP isoform higher than 70 %. Low inhibition of CYP2D6 and moderate inhibition of CYP2C19 was observed. At the same concentration, 2-ethylimidazole **20c** shows both a higher inhibition of hERG (43 %) and an elevated CYP inhibition profile than the 2-methylsufanylimidazole counterpart **1c**. This finding is in good agreement with recently reported results of a study with similar imidazole derivatives.[49]

The water solubility of dual GSK3β/p38α MAP kinase inhibitors **1c** and **20c** was measured in PBS buffer at a pH value of 7.8 (Figures S1 and S2, supplementary data). While 2-methylsulfanylimidazole **1c** showed moderate solubility (0.051 mg/mL), the 2-ethylimidazole **20c** displayed a 3-fold improved solubility (0.155 mg/mL).

Finally, compound **20c** was further screened against a panel of 45 diverse kinases in order to achieve a preliminary evaluation of its selectivity within the kinome. Ten additional kinases were inhibited more than 60 % at a testing concentration of 1 µM apart from GSK3β and p38α MAPK (Table 7 and Table S4, supplementary data). Among these, the tyrosine kinase receptors VEGFR2, EGFR, FGRF2 and FGFR3 were found as targets. Also, the p38α MAPK-related kinase JNK1 was identified as an off-target.

Table 7. Off target activity of **20c** (test concentration: 1 µM).

90-100% inhibition	**75-90% inhibition**	**60-75% inhibition**
Abl	EPHA2	EPHA3
EGFR	JNK1	FGFR2
EphB4		
FGFR3		
HGK (MAP4K4)		

KDR (VEGFR2)

3. Conclusion

A comprehensive series of 2,4,5-trisubstituted imidazoles was synthesized and biologically evaluated, providing for the first-time valuable insights into the SARs of this class of compounds with respect to their p38α MAP kinase and GSK3β inhibitory potencies. Structural modifications led to promising inhibitors targeting simultaneously both kinases relevant for the pathophysiology of AD. The most promising balanced dual inhibitor *N*-(4-(2-ethyl-4-(4-fluorophenyl)-1*H*-imidazol-5-yl)pyridin-2-yl)cyclopropanecarboxamide (**20c**) displayed IC_{50} values in the low double-digit nanomolar range and shows excellent metabolic stability. In addition to this, compound **20c** demonstrated an 8.5-fold isoform selectivity over GSK3α and seems to possess favourable pharmacokinetic properties, like the ability to cross the blood-brain barrier in mice.

4. Experimental section

4.1. Chemistry

4.1.1. General

All reagents were obtained from commercial sources and used without further purification. All solvents were purchased from Acros in anhydrous, extra dry (over molecular sieves) quality and used as received unless otherwise stated. Thin layer chromatography (TLC) reaction controls were performed for all reactions using fluorescent silica gel 60 F_{254} plates (Merck) and visualized under natural light and UV illumination at 254 and 366 nm. All tested compounds were determined to be ≥95 % purity by reverse phase high-performance liquid chromatography (HPLC) (254 nm). HPLC were carried out on an

587 Agilent 1100 Series HPLC system, equipped with an UV DAD (detection at 218 nm, 254
588 nm, and 280 nm). The chromatographic separation was performed on a XBridge^{TM} C18
589 column (150 mm x 4.6 mm, 5 µm) at 30 °C oven temperature. The injection volume was
590 10 µL and the flow 1.5 mL / min using the following gradient: 0.01 M KH_2PO_4, pH 2.3
591 (solvent A), methanol (solvent B), 45 % B to 85 % B in 9 min; 85 % B for 6 min; stop time
592 16 min. Flash column chromatography was performed using an Interchim PuriFlash 430
593 automated flash chromatography system with Davisil LC60A 20 - 45 µm silica from Grace
594 Davison or PuriFlash SIHP 30 µm columns. Nuclear magnetic resonance (NMR) spectra
595 were measured on a Bruker Avance III HD NMR spectrometer at 300 MHz in the Organic
596 Chemistry Institute, Eberhard Karls Universität Tübingen. The chemical shifts δ are
597 reported in parts per million (ppm) relative to TMS. All spectra were calibrated against the
598 (residual proton) peak of the deuterated solvent used. Mass spectra were performed on an
599 Advion Expression S electrospray ionization mass spectrometer (ESI-MS) with an Advion
600 Plate Express (TLC interface).
601
602 *4.2. Experimental procedures*
603 *4.2.1. General Procedure for the Buchwald-Hartwig Coupling (General Procedure A)*
604 The amide (1.5 – 3 equiv), $Pd_2(dba)_3$ (5 mol %), XantPhos (10 mol %), cesium carbonate
605 (3 equiv) and the 2-chloropyridinylimidazole derivative (**11a** or **11b**) were dissolved under
606 an atmosphere of argon in DMF (6.5 mL/mmol). The reaction mixture was then stirred at
607 100 °C for 16 h. The reaction mixture was allowed to cool to rt and sat. ammonium
608 chloride solution was added. It was extracted with ethyl acetate (3x) and the combined
609 organic layers were washed with sat. ammonium chloride solution (2x) and brine. After
610 drying over anhydrous Na_2SO_4 the solvent was evaporated under reduced pressure.

4.2.2. General Procedure for the Amide Coupling with PyBOP (General Procedure B)

The carboxylic acid (1 – 2.5 equiv) and (benzotriazol-1-yloxy)tripyrrolidinophosphonium hexafluorophosphate (PyBOP) (1 – 2.5 equiv) were dissolved in DCM (25 mL/mmol). The resulting mixture was stirred for 10 min at rt before the amine (1 equiv) and diisopropylethylamine (3 equiv) were added. The reaction was stirred overnight at rt. The solvent was evaporated under reduced pressure and the residue was dissolved in DCM and washed with brine and sat. sodium bicarbonate solution. The organic layer was dried over anhydrous Na_2SO_4 before the solvent was again evaporated under reduced pressure.

4.2.3. General Procedure for the Amide Coupling with HATU (General Procedure C)

The carboxylic acid (1 – 3 equiv) and 1-[bis(dimethylamino)methylene]-1*H*-1,2,3-triazolo[4,5-*b*]pyridinium 3-oxide hexafluorophosphate (HATU) (1 – 1.4 equiv) were dissolved in DCM (25 mL/mmol). The resulting mixture was stirred for 10 min at rt before the amine (1 equiv) was added and the mixture was stirred for 20 more min. Then diisopropylethylamine (3 equiv) was added and the reaction was stirred overnight at rt. The solvent was evaporated under reduced pressure and the residue was dissolved in DCM and washed with brine and sat. sodium bicarbonate solution. The organic layer was dried over anhydrous Na_2SO_4 before the solvent was again evaporated under reduced pressure.

4.2.4. General Procedure for the Radziszewski Imidazole Synthesis (General Procedure D)

The diketone **19a** was dissolved in acetic acid (20 mL/mmol) and ammonium acetate (20 equiv) and the aldehyde (1.5 equiv) were added. The reaction mixture was heated to 130 °C for 4 h. After cooling to rt, the reaction was diluted with DCM and sat. sodium bicarbonate solution was added until gas evolution ceased. The phases were separated and the aqueous layer was adjusted to pH 10-11 with 1 M NaOH and extracted thrice with DCM.

*4.2.5.1. tert-Butyl (4-methoxybenzyl)(4-methylpyridin-2-yl)carbamate (**4**)*

A solution of *tert*-butyl (4-methylpyridin-2-yl)carbamate (2.00 g, 9.60 mmol) in DMF (20 mL) was cooled to 0 °C and sodium hydride 60 % in mineral oil (576 mg, 14.40 mmol) was added portionwise over 5 min. The resultant mixture was stirred for 30 min at 0 °C before 4-methoxybenzyl chloride (1.56 mL, 11.52 mmol) was added in one portion and the reaction was stirred at rt for 18 h. Water (200 mL) was added and it was extracted with ethyl acetate (3x). The combined organic layers were dried over anhydrous Na_2SO_4 and concentrated in vacuo to afford a brown solid (3.27 g), which was used in the next step without further purification. ^{1}H NMR (300 MHz, $CDCl_3$) δ 1.43 (s, 9H), 2.33 (s, 3H), 3.77 (s, 3H), 5.11 (s, 2H), 6.76 - 6.87 (m, 3H), 7.17 - 7.25 (m, 2H), 7.45 (s, 1H), 8.25 (d, *J* = 5.0 Hz, 1H). ^{13}C NMR (75 MHz, $CDCl_3$) δ 21.1, 28.2, 49.4, 55.7, 81.1, 113.5, 120.3, 120.8, 128.6, 131.6, 147.2, 148.1, 154.3, 154.5, 158.4. TLC-MS (ESI) *m*/*z* = 350.8 $[M + Na]^+$.

*4.2.5.2. tert-Butyl (4-(2-(4-fluorophenyl)-2-oxoethyl)pyridin-2-yl)(4-methoxybenzyl)carbamate (**5**)*

Under an atmosphere of argon, compound **4** (1.41 g, 4.29 mmol) was dissolved in THF (35 mL) and the solution was cooled to 0 °C. Sodium bis(trimethylsilyl)amide(4.30 mL, 8.60 mmol, 2 M in THF) was added via syringe over 10 min and the resulting mixture was stirred for 45 min while still being cooled to 0 °C. Then ethyl 4-fluorobenzoate (867 mg, 5.16 mmol) dissolved in THF (5 mL) was added in one portion and the reaction was further stirred for 2 h at rt. H_2O (150 mL) was added and the solution was carefully adjusted to pH = 7 using 0.5 M aqueous HCl. The organic layer was separated and the aqueous layer was extracted with ethyl acetate (2x). The combined organic layers were dried over anhydrous Na_2SO_4 and concentrated in vacuo to afford a brown solid (1.24 g, 67 % over 2 steps). ^{1}H NMR (300 MHz, DMSO-d_6) δ 1.36 (s, 9H), 3.70 (s, 3H), 4.47 (s, 2H), 5.02 (s, 2H), 6.79 - 6.86 (m, 2H), 7.04 (dd, *J* = 5.1, 1.3 Hz, 1H), 7.13 - 7.19 (m, 2H), 7.30 - 7.41 (m, 2H), 7.50 (s, 1H), 8.08 - 8.16 (m, 2H), 8.30 (dd, *J* = 5.1, 0.4 Hz, 1H). ^{13}C NMR (75 MHz,

662 $CDCl_3$) δ 27.7, 43.9, 48.8, 54.9, 80.6, 113.5, 115.8 (d, $^2J_{CF}$ = 22.1 Hz), 120.7, 121.6, 128.3,
663 130.9, 131.3 (d, $^3J_{CF}$ = 9.4 Hz), 133.0 (d, $^4J_{CF}$ = 2.8 Hz), 145.4, 147.1, 153.4, 154.0, 158.1,
664 165.2 (d, $^1J_{CF}$ = 252.1 Hz), 195.1. TLC-MS (ESI) *m/z* = 473.2 $[M + Na]^+$.

665 *4.2.5.3. tert-Butyl-(4-(2-(4-fluorophenyl)-1-(hydroxyimino)-2-oxoethyl)pyridin-2-yl)(4-*
666 *methoxybenzyl)carbamate (**6**)*

667 Sodium nitrite (483 mg, 7.00 mmol) was dissolved in H_2O (5 mL) and added dropwise to a
668 solution of **5** (1.05 g, 2.33 mmol) in glacial acetic acid (15 mL) at 10 °C. The resulting
669 mixture was stirred for 60 min before H_2O (50 mL) was added and the aqueous phase was
670 extracted with ethyl acetate (3x). The combined organic layers were dried over anhydrous
671 Na_2SO_4 and concentrated in vacuo to afford an orange-brown solid (1.12 g, 100 %). ^1H
672 NMR (300 MHz, $CDCl_3$) δ 1.36 (s, 9H), 3.75 (s, 3H), 5.08 (s, 2H), 6.73 - 6.79 (m, 2H), 7.08
673 - 7.13 (m, 2H), 7.14 - 7.17 (m, 2H), 7.18 (d, *J* = 2.7 Hz, 1H), 7.76 (s, 1H), 7.89 - 7.97 (m,
674 2H), 8.35 (d, *J* = 5.3 Hz, 1H). ^{13}C NMR (75 MHz, $CDCl_3$) δ 28.0, 49.7, 55.1, 81.9, 113.5,
675 116.3, 116.4 (d, $^2J_{CF}$ = 22.7 Hz), 116.8, 128.6, 130.6, 131.0 (d, $^4J_{CF}$ = 2.8 Hz), 132.2 (d,
676 $^3J_{CF}$ = 9.4 Hz), 140.3, 148.0, 153.8, 154.1, 154.9, 158.4, 166.6 (d, $^1J_{CF}$ = 257.6 Hz), 192.1
677 TLC-MS (ESI) *m/z* = 502.0 $[M + Na]^+$ *m/z* = 478.1 $[M - H]^-$.

678 *4.2.5.4. 2-Amino-1-(4-fluorophenyl)-2-(2-((4-methoxybenzyl)amino)pyridin-4-yl)ethan-1-*
679 *one-hydrochloride (**7**)*

680 In a three-neck round-bottom flask, compound **6** (1.12 g, 2.33 mmol) was dissolved in a
681 1:1 mixture of methanol (15 mL) and hydrochloric acid in methanol (15 mL). Palladium on
682 carbon 10 wt. % (250 mg) was added and the flask was evacuated and backfilled with
683 hydrogen gas. The reaction was carefully heated to 45 °C and vigorously stirred for 6 h
684 under an atmosphere of hydrogen. The reaction mixture was filtered through Celite and
685 the solvent was evaporated to give **7** as a yellow solid (904 mg), which was used in the

next step without further purification. TLC-MS (ESI) *m*/*z* = 366.3 $[M + H]^+$ *m*/*z* = 364.3 $[M - H]^-$.

*4.2.5.5. 4-(4-Fluorophenyl)-5-(2-((4-methoxybenzyl)amino)pyridin-4-yl)-1,3-dihydro-2H-imidazole-2-thione (**8**)*

Compound **7** (1.00 g, 2.49 mmol) and potassium thiocyanate (532 mg, 5.47 mmol) were dissolved in DMF (7 mL) under an atmosphere of argon and stirred at 160 °C for 2 h. After cooling to rt, H_2O (75 ml) was added and the precipitate was filtered off and dried in vacuo to afford **8** as a yellow solid (644 mg, 62 % over 2 steps). ^{1}H NMR (300 MHz, DMSO-d_6) δ 3.73 (s, 3H), 4.35 (d, *J* = 5.2 Hz, 2H), 6.45 (d, *J* = 5.0 Hz, 1H), 6.60 (s, 1H), 6.89 (d, *J* = 8.5 Hz, 2H), 7.16 - 7.33 (m, 5H), 7.46 (dd, *J* = 8.6, 5.4 Hz, 2H), 7.88 (d, *J* = 5.6 Hz, 1H), 12.70 (d, *J* = 5.2 Hz, 2H). TLC-MS (ESI) *m*/*z* = 407.6 $[M + H]^+$ *m*/*z* = 405.3 $[M - H]^-$.

*4.2.5.6. 4-(5-(4-Fluorophenyl)-2-(methylthio)-1H-imidazol-4-yl)-N-(4-methoxybenzyl)pyridin-2-amine (**9a**)*

Compound **8** (644 mg, 1.58 mmol) was dissolved in methanol (12 mL) and cooled to 0 °C before sodium *tert*-butoxide (305 mg, 3.17 mmol) and methyl iodide (100 µL, 1.60 mmol) were added. The reaction was stirred at 55 °C for 2 h. Afterwards the solvent was evaporated and the crude product was purified by flash column chromatography (SiO_2, DCM/EtOH 97:03 to 85:15) to afford a brown solid (560 mg, 84 %). ^{1}H NMR (300 MHz, DMSO-d_6) δ 2.60 (s, 3H), 3.72 (s, 3H), 4.33 (d, *J* = 5.5 Hz, 2H), 6.47 (d, *J* = 4.7 Hz, 1H), 6.70 (br. s., 1H), 6.81 - 6.89 (m, 2H), 6.96 - 7.08 (m, 1H), 7.19 (d, *J* = 8.5 Hz, 3H), 7.28 (t, *J* = 8.6 Hz, 1H), 7.40 - 7.56 (m, 2H), 7.73 - 8.00 (m, 1H), 12.60 (br. s., 1H). TLC-MS (ESI) *m*/*z* = 421.2 $[M + H]^+$ *m*/*z* = 419.0 $[M - H]^-$.

*4.2.5.7. 4-(2-(Benzylthio)-5-(4-fluorophenyl)-1H-imidazol-4-yl)-N-(4-methoxybenzyl)pyridin-2-amine (**9b**)*

Compound **8** (1.00 g, 2.46 mmol) was dissolved in DMF (6 mL) before cesium carbonate (425 mg, 3.08 mmol) and benzyl bromide (290 µL, 2.46 mmol) were added. The reaction was stirred at rt for 36 h, before water (50 ml) was added and it was extracted with ethyl acetate (3x). The combined organic layers were dried over anhydrous Na_2SO_4, concentrated in vacuo and purified by flash column chromatography (SiO_2, DCM/EtOH 97:03 to 85:15) to yield **9b** as a brown oil (435 mg, 35 %). ^{1}H NMR (300 MHz, DMSO-d_6) δ 3.71 (s, 3H), 4.25 - 4.49 (m, 4H), 6.49 (br. s., 1H), 6.73 (br. s., 1H), 6.86 (d, *J* = 8.1 Hz, 2H), 7.02 (d, *J* = 15.9 Hz, 1H), 7.11 - 7.60 (m, 11H), 7.74 - 8.01 (m, 1H), 12.69 (br. s., 1H). TLC-MS (ESI) *m*/*z* = 497.3 $[M + H]^+$ *m*/*z* = 495.4 $[M - H]^-$.

*4.2.5.8. 4-(5-(4-Fluorophenyl)-2-(methylthio)-1H-imidazol-4-yl)pyridin-2-amine (**10a**)*

Compound **9a** (650 mg, 1.55 mmol) was dissolved in TFA (6 mL) and heated to 55 °C until reaction control by TLC showed complete conversion. The solvent was evaporated and the product was redissolved in ethyl acetate and then washed with sat. sodium bicarbonate solution (2x). Purification by flash column chromatography (SiO_2, DCM/EtOH 95:05 to 90:10) afforded a golden solid (451 mg, 97 %). ^{1}H NMR (300 MHz, DMSO-d_6) δ 2.61 (s, 3H), 5.98 (br. s., 2H), 6.45 (dd, *J* = 5.4, 1.5 Hz, 1H), 6.72 (br. s., 1H), 7.10 - 7.36 (m, 2H), 7.48 (br. s., 2H), 7.69 - 7.92 (m, 1H), 12.62 (br. s., 1H). TLC-MS (ESI) *m*/*z* = 301.4 $[M + H]^+$ *m*/*z* = 299.2 $[M - H]^-$.

*4.2.5.9. 4-(2-(Benzylthio)-5-(4-fluorophenyl)-1H-imidazol-4-yl)pyridin-2-amine (**10b**)*

Compound **9b** (398 mg, 0.80 mmol) was dissolved in TFA (6 mL) and heated to 55 °C until reaction control by TLC showed complete conversion. The solvent was evaporated and the product was redissolved in ethyl acetate and then washed with sat. sodium bicarbonate solution (2x). Purification by flash column chromatography (SiO_2, DCM/EtOH 95:05 to 90:10) afforded a brown solid (289 mg, 96 %). ^{1}H NMR (300 MHz, DMSO-d_6) δ

4.38 (s, 2H), 5.94 (br. s., 2H), 6.44 (d, *J* = 4.6 Hz, 1H), 7.11 - 7.56 (m, 10H), 7.68 - 7.91 (m, 1H), 12.71 (br. s., 1H); TLC-MS (ESI) *m*/*z* = 377.2 $[M + H]^+$ *m*/*z* = 375.3 $[M - H]^-$.

*4.2.5.10. N-(4-(5-(4-Fluorophenyl)-2-(methylthio)-1H-imidazol-4-yl)pyridin-2-yl)-3-(3,4,5-trimethoxyphenyl)propanamide (**1a**)*[27]

The title compound was prepared according to **general procedure B** starting from **10a** (50 mg, 0.17 mmol) and 3-(3,4,5-trimethoxyphenyl)propionic acid (52 mg, 0.22 mmol). Purification by flash column chromatography (SiO_2, DCM/EtOH 97:03) afforded **1a** as a yellow solid (35 mg, 40 %). ^{1}H NMR (300 MHz, $CDCl_3$) δ 2.63 (s, 3H), 2.64 - 2.70 (m, 2H), 2.88 - 2.97 (m, 2H), 3.77 (s, 6H), 3.79 (s, 3H), 6.38 (s, 2H), 6.92 - 7.10 (m, 3H), 7.32 - 7.46 (m, 2H), 8.00 (d, *J* = 5.4 Hz, 1H), 8.31 (br. s., 1H), 8.71 (br. s., 1H). ^{13}C NMR (75 MHz, $CDCl_3$) δ 16.1, 31.7, 39.4, 56.1, 60.8, 105.3, 111.4, 115.8 (d, $^2J_{CF}$ = 22.1 Hz), 117.7, 130.2 (d, $^3J_{CF}$ = 7.7 Hz), 136.2, 136.4, 147.5, 151.6, 153.2, 162.6 (d, $^1J_{CF}$ = 248.0 Hz); TLC-MS (ESI) *m*/*z* = 545.7 $[M + Na]^+$ *m*/*z* = 521.4 $[M - H]^-$. HPLC: t_R = 7.55 min (96.3 % purity).

*4.2.5.13. N-(4-(5-(4-Fluorophenyl)-2-(methylthio)-1H-imidazol-4-yl)pyridin-2-yl)acetamide (**1b**)[50]*

The title compound was prepared according to **general procedure A** starting from **11a** (200 mg, 0.63 mmol) and acetamide (111 mg, 1.89 mmol). Purification by flash column chromatography (SiO_2, DCM/EtOH 96:04) afforded **1b** as a yellow solid (118 mg, 55 %). ^{1}H NMR (300 MHz, DMSO-d_6) δ 2.03 - 2.09 (m, 3H), 2.62 (s, 3H), 6.98 - 7.09 (m, 1H), 7.17 (s, 1H), 7.29 (t, *J* = 8.9 Hz, 1H), 7.43 - 7.55 (m, 2H), 8.13 (d, *J* = 5.4 Hz, 1H), 8.29 (s, 1H), 10.33 (s, 1H), 12.71 (br. s., 1H). ^{13}C NMR (75 MHz, DMSO-d_6) δ 15.2, 23.9, 110.4, 115.9 (d, $^2J_{CF}$ = 21.5 Hz), 116.5, 126.6 (d, $^4J_{CF}$ = 3.3 Hz), 130.1, 130.7 (d, $^3J_{CF}$ = 8.3 Hz), 134.5, 142.2, 143.8, 147.7, 152.5, 162.0 (d, $^1J_{CF}$ = 245.5 Hz), 169.0. TLC-MS (ESI) *m*/*z* = 343.3 $[M + H]^+$ *m*/*z* = 341.1 $[M - H]^-$. HPLC: t_R = 3.60 min (96.7 % purity)

*4.2.5.14. N-(4-(4-(4-Fluorophenyl)-2-(methylthio)-1H-imidazol-5-yl)pyridin-2-yl)cyclopropanecarboxamide (**1c**)*

The title compound was prepared according to **general procedure A** starting from **11a** (200 mg, 0.63 mmol) and cyclopropanecarboxamide (40 mg, 0.47 mmol). Purification by flash column chromatography (SiO_2, *n*-hexane/EtOAc 70:30 to 20:80) afforded **1c** as a yellow solid (43 mg, 42 %). ^{1}H NMR (300 MHz, DMSO-d_6) δ 0.78 (d, J = 5.9 Hz, 4H), 1.93 - 2.04 (m, 1H), 2.62 (s, 3H), 6.97 (dd, J = 5.3, 1.6 Hz, 1H), 7.12 - 7.33 (m, 2H), 7.43 - 7.54 (m, 2H), 8.11 (d, J = 5.2 Hz, 1H), 8.34 (s, 1H), 10.60 - 10.84 (m, 1H), 12.66 - 12.82 (m, 1H). ^{13}C NMR (75 MHz, DMSO-d_6) δ 7.5, 14.2, 15.1, 110.6, 115.8 (d, $^2J_{CF}$ = 21.5 Hz), 116.3, 126.6 (d, $^4J_{CF}$ = 3.3 Hz), 130.0, 130.7 (d, $^3J_{CF}$ = 8.3 Hz), 134.5, 142.2, 143.8, 147.6, 152.5, 161.9 (d, $^1J_{CF}$ = 247.1 Hz), 172.3. TLC-MS (ESI) m/z = 369.1 $[M + H]^+$ m/z = 366.9 $[M-H]^-$. HPLC: t_R = 5.16 min (97.4 % purity)

*4.2.5.11. N-(4-(5-(4-Fluorophenyl)-2-(methylthio)-1H-imidazol-4-yl)pyridin-2-yl)cyclopentanecarboxamide (**1d**)*

The title compound was prepared according to **general procedure B** starting from **10a** (93 mg, 0.31 mmol) and cyclopentanecarboxylic acid (46 mg, 0.40 mmol). Purification by flash column chromatography (SiO_2, DCM/EtOH 97:03) afforded **1d** as a yellow solid (60 mg, 49 %). ^{1}H NMR (300 MHz, DMSO-d_6) δ 1.46 - 1.58 (m, 2H), 1.60 - 1.73 (m, 4H), 1.75 - 1.90 (m, 2H), 2.62 (s, 3H), 2.83 - 2.99 (m, 1H), 6.97 (dd, J = 5.3, 1.6 Hz, 1H), 7.25 (br. s., 2H), 7.42 - 7.56 (m, 2H), 8.15 (br. s., 1H), 8.31 (br. s., 1H), 10.34 (br. s., 1H), 12.74 (br. s, 1H). ^{13}C NMR (75 MHz, $CDCl_3$) δ 16.0, 25.9, 30.2, 45.3, 111.1, 115.7 (d, $^2J_{CF}$ = 22.1 Hz), 117.2, 130.2 (d, $^3J_{CF}$ = 7.7 Hz), 146.2, 152.0, 162.6 (d, $^1J_{CF}$ = 248.2 Hz), 181.7. TLC-MS (ESI) m/z = 397.2 $[M + H]^+$ m/z = 395.2 $[M - H]^-$. HPLC: t_R = 7.12 min (97.0 % purity).

*4.2.5.12. N-(4-(5-(4-Fluorophenyl)-2-(methylthio)-1H-imidazol-4-yl)pyridin-2-yl)-2-(3,4,5-trimethoxyphenyl)acetamide (**1e**)*

The title compound was prepared according to **general procedure B** starting from **10a** (72 mg, 0.24 mmol) and 2-(3,4,5-trimethoxyphenyl)acetic acid (136 mg, 0.6 mmol). Purification

785 by flash column chromatography (SiO_2, DCM/EtOH 97:03) afforded **1e** as a yellow solid
786 (88 mg, 77 %). ^{1}H NMR (300 MHz, $CDCl_3$) δ 2.59 (s, 3H), 3.61 (s, 2H), 3.77 (s, 6H), 3.80
787 (s, 3H), 6.45 (s, 2H), 6.96 (t, *J* = 8.7 Hz, 2H), 7.05 (d, *J* = 4.9 Hz, 1H), 7.35 (dd, *J* = 8.5, 5.5
788 Hz, 2H), 8.02 (d, *J* = 5.4 Hz, 1H), 8.33 (s, 1H), 8.48 (br. s., 1H). ^{13}C NMR (75 MHz, $CDCl_3$)
789 δ 16.1, 45.0, 56.1, 60.8, 106.4, 111.3, 115.7 (d, $^2J_{CF}$ = 21.6 Hz), 117.9, 129.4, 130.2 (d,
790 $^3J_{CF}$ = 7.7 Hz), 137.3, 143.5, 147.5, 151.5, 153.6, 162.5 (d, $^1J_{CF}$ = 248.2 Hz), 169.8. TLC-
791 MS (ESI) *m*/*z* = 508.9 $[M + H]^+$ *m*/*z* = 507.1 $[M - H]^-$. HPLC: t_R = 6.20 min (100.0 % purity).

792 *4.2.5.13. N-(4-(5-(4-Fluorophenyl)-2-(methylthio)-1H-imidazol-4-yl)pyridin-2-yl)-3-(4-*
793 *methoxyphenyl)propanamide (**1f**)*

794 The title compound was prepared according to **general procedure B** starting from **10a** (72
795 mg, 0.24 mmol) and 3-(4-methoxyphenyl)propionic acid (108 mg, 0.60 mmol). Purification
796 by flash column chromatography (SiO_2, DCM/EtOH 97:03) afforded **1f** as a yellow solid
797 (50 mg, 45 %). ^{1}H NMR (300 MHz, $CDCl_3$) δ 2.55 - 2.71 (m, 5 H), 2.91 (t, *J* = 7.7 Hz, 2H),
798 3.75 (s, 3H), 6.75 - 6.82 (m, 2H), 6.95 - 7.11 (m, 5 H), 7.40 (dd, *J* = 8.1, 5.5 Hz, 2H), 7.97
799 (d, *J* = 5.5 Hz, 1H), 8.33 (s, 1H), 9.00 (br. s., 1H). ^{13}C NMR (75 MHz, $CDCl_3$) δ 16.1, 30.3,
800 39.4, 55.2, 111.3, 113.9, 115.7 (d, $^2J_{CF}$ = 21.6 Hz), 117.5, 129.2, 130.2 (d, $^3J_{CF}$ = 8.3 Hz),
801 132.3, 147.0, 151.6, 158.0, 162.6 (d, $^1J_{CF}$ = 248.2 Hz), 171.4; TLC-MS (ESI) *m*/*z* = 462.8
802 $[M + H]^+$ *m*/*z* = 461.0 $[M - H]^-$. HPLC: t_R = 7.56 min (99.5 % purity).

803 *4.2.5.14. N-(4-(5-(4-Fluorophenyl)-2-(methylthio)-1H-imidazol-4-yl)pyridin-2-yl)-3-(3-*
804 *methoxyphenyl)propanamide (**1g**)*

805 The title compound was prepared according to **general procedure B** starting from **10a** (72
806 mg, 0.24 mmol) and 3-(3-methoxyphenyl)propionic acid (108 mg, 0.60 mmol). Purification
807 by flash column chromatography (SiO_2, DCM/EtOH 97:03) afforded **1f** as a yellow solid
808 (73 mg, 66 %). ^{1}H NMR (300 MHz, $CDCl_3$) δ 2.61 (s, 3H), 2.65 (d, *J* = 8.0 Hz, 2H), 2.93 (t,
809 *J* = 7.3 Hz, 2H), 3.73 (s, 3H), 6.67 - 6.75 (m, 3H), 6.94 - 7.05 (m, 3H), 7.11 - 7.18 (m, 1H),
810 7.38 (dd, *J* = 8.2, 5.6 Hz, 2H), 7.97 (d, *J* = 5.3 Hz, 1H), 8.32 (br. s., 1H), 9.12 (br. s., 1H).

^{13}C NMR (75 MHz, $CDCl_3$) δ 16.1, 45.0, 56.1, 60.8, 106.4, 111.3, 115.7 (d, $^2J_{CF}$ = 21.6 Hz), 117.9, 129.4, 130.2 (d, $^3J_{CF}$ = 7.7 Hz), 137.3, 143.5, 147.5, 151.5, 153.6, 162.5 (d, $^1J_{CF}$ = 248.2 Hz), 170.6; TLC-MS (ESI) *m*/*z* = 462.9 $[M + H]^+$ *m*/*z* = 461.1 $[M - H]^-$. HPLC: t_R = 7.74 min (100.0 % purity).

*4.2.5.15. N-(4-(5-(4-Fluorophenyl)-2-(methylthio)-1H-imidazol-4-yl)pyridin-2-yl)-2-(4-(trifluoromethyl)phenyl)acetamide (**1h**)*

The title compound was prepared according to **general procedure C** starting from **10a** (36 mg, 0.12 mmol) and 4-(trifluoromethyl)phenylacetic acid (31 mg, 0.15 mmol). Purification by flash column chromatography (SiO_2, *n*-hexane/EtOAc 50:50) afforded **1h** as a yellow solid (43 mg, 73 %). ^{1}H NMR (300 MHz, DMSO-d_6) δ 2.61 (s, 3H), 3.18 (s, 2H), 7.02 (dd, *J* = 5.3, 1.6 Hz, 1H), 7.23 (t, *J* = 8.8 Hz, 2H), 7.43 - 7.51 (m, 2H), 7.56 (d, *J* = 8.1 Hz, 2H), 7.69 (d, *J* = 8.1 Hz, 2H), 8.18 (d, *J* = 5.2 Hz, 1H), 8.26 (s, 1H), 10.75 (s, 1H), 12.72 (br. s., 1H). ^{13}C NMR (101 MHz, DMSO-d_6) δ 15.0, 42.6, 110.6, 115.6 (d, $^2J_{CF}$ = 22.0 Hz), 116.8, 124.3 (q, $^1J_{CF3}$ = 272.2 Hz), 125.0 (q, $^3J_{CF3}$ = 3.7 Hz), 127.3 (q, $^2J_{CF3}$ = 31.5 Hz), 129.9, 130.3 (d, $^3J_{CF}$ = 8.3 Hz), 140.6, 142.6, 147.7, 152.3, 161.8 (d, $^1J_{CF}$ = 245.2 Hz), 169.0. TLC-MS (ESI) *m*/*z* = 487.3 $[M + H]^+$ *m*/*z* = 485.2 $[M - H]^-$. HPLC: t_R = 8.85 min (100.0 % purity)

*4.2.5.16. N-(4-(5-(4-Fluorophenyl)-2-(methylthio)-1H-imidazol-4-yl)pyridin-2-yl)-3-(4-(trifluoromethyl)phenyl)propanamide (**1i**)*

The title compound was prepared according to **general procedure B** starting from **10a** (72 mg, 0.24 mmol) and 3-[4-(trifluoromethyl)phenyl]propionic acid (78 mg, 0.36 mmol). Purification by flash column chromatography (SiO_2, *n*-hexane/EtOAc 50:50) afforded **1i** as a yellow solid (49 mg, 41 %). ^{1}H NMR (300 MHz, $CDCl_3$) δ 2.63 (s, 3H), 2.70 (t, *J* = 7.4 Hz, 2H), 2.98 - 3.06 (m, 2H), 7.00 (t, *J* = 8.6 Hz, 2H), 7.09 (d, *J* = 4.9 Hz, 1H), 7.27 (d, *J* = 8.0 Hz, 2H), 7.38 (dd, *J* = 8.3, 5.4 Hz, 2H), 7.50 (d, *J* = 8.0 Hz, 2H), 7.97 (d, *J* = 5.3 Hz, 1H),

8.29 (br. s., 1H), 9.09 (br. s., 1H). ^{13}C NMR (75 MHz, $CDCl_3$) δ 16.1, 30.6, 38.3, 111.2, 115.8 (d, $^{2}J_{CF}$ = 22.1 Hz), 117.5, 124.2 (q, $^{1}J_{CF3}$ = 271.4 Hz), 125.4 (q, $^{3}J_{CF3}$ = 3.9 Hz), 128.6 (q, $^{2}J_{CF3}$ = 32.6 Hz), 128.7, 130.2 (d, $^{3}J_{CF}$ = 8.3 Hz), 143.8, 144.4, 146.2, 151.2, 162.7 (d, $^{1}J_{CF}$ = 248.8 Hz), 170.8. TLC-MS (ESI) *m*/*z* = 501.0 $[M + H]^+$ *m*/*z* = 499.1 $[M - H]^-$. HPLC: t_R = 9.32 min (97.1 % purity).

*4.2.5.17. N-(4-(5-(4-Fluorophenyl)-2-(methylthio)-1H-imidazol-4-yl)pyridin-2-yl)-1-(trifluoromethyl)cyclopropane-1-carboxamide (**1j**)*

The title compound was prepared according to **general procedure C** starting from **10a** (72 mg, 0.24 mmol) and 1-(trifluoromethyl)cyclopropane-1-carboxylic acid (51 mg, 0.33 mmol). Purification by flash column chromatography (SiO_2, *n*-hexane/EtOAc 50:50) afforded **1j** as a yellow solid (43 mg, 41 %). ^{1}H NMR (300 MHz, $CDCl_3$) δ 1.30 - 1.37 (m, 2H), 1.45 - 1.53 (m, 2H), 2.64 (d, *J* = 3.9 Hz, 3H), 6.97 - 7.10 (m, 3H), 7.33 - 7.43 (m, 2H), 8.10 (d, *J* = 5.3 Hz, 1H), 8.22 (s, 1H), 8.40 (br. s., 1H). ^{13}C NMR (75 MHz, $CDCl_3$) δ 12.6, 16.2, 28.6 (q, $^{2}J_{CF3}$ = 33.7 Hz), 111.4, 115.9 (d, $^{2}J_{CF}$ = 21.6 Hz), 118.1, 125.4 (q, $^{1}J_{CF3}$ = 273.1 Hz), 130.2 (d, $^{3}J_{CF}$ = 8.3 Hz), 143.4, 147.8, 151.1, 162.7 (d, $^{1}J_{CF}$ = 248.8 Hz), 164.6. TLC-MS (ESI) *m*/*z* = 437.2 $[M + H]^+$ *m*/*z* = 435.3 $[M - H]^-$. HPLC: t_R = 8.04 min (97.6 % purity)

*4.2.5.18. trans-N-(4-(5-(4-Fluorophenyl)-2-(methylthio)-1H-imidazol-4-yl)pyridin-2-yl)-2-phenylcyclopropane-1-carboxamide (**1k**)*

The title compound was prepared according to **general procedure C** starting from **10a** (53 mg, 0.18 mmol) and *trans*-2-phenylcyclopropane-1-carboxylic acid[51] (43 mg, 0.27 mmol). Purification by flash column chromatography (SiO_2, DCM/EtOH 97:03) afforded **1k** as a semi-white solid (30 mg, 38 %). ^{1}H NMR (300 MHz, $CDCl_3$) δ 1.35 (ddd, *J* = 8.0, 6.6, 4.6 Hz, 1H), 1.67 (dt, *J* = 9.4, 4.7 Hz, 1H), 1.78 - 1.88 (m, 1H), 2.49 - 2.59 (m, 1H), 2.64 (s, 3H), 6.89 - 6.96 (m, 1H), 6.98 - 7.10 (m, 4H), 7.14 - 7.29 (m, 3H), 7.34 - 7.50 (m, 2H), 7.90 (d, *J* = 5.4 Hz, 1H), 8.34 (s, 1H), 9.29 (br. s., 1H). ^{13}C NMR (75 MHz, $CDCl_3$) δ 16.1, 16.6, 26.5, 27.5, 111.1, 115.8 (d, $^{2}J_{CF}$ = 21.6 Hz), 117.4, 126.0, 126.5, 128.5, 130.1 (d, $^{3}J_{CF}$ =

8.3 Hz), 140.0, 143.7, 147.4, 151.9, 162.6 (d, $^{1}J_{CF}$ = 248.2 Hz), 171.0. TLC-MS (ESI) *m/z* 444.9 $[M + H]^+$ *m/z* = 443.0 $[M - H]^-$. HPLC: t_R = 8.67 min (100.0 % purity).

*4.2.5.19. 2-Cyclopropyl-N-(4-(5-(4-fluorophenyl)-2-(methylthio)-1H-imidazol-4-yl)pyridin-2-yl)acetamide (**1l**)*

The title compound was prepared according to **general procedure B** starting from **10a** (72 mg, 0.24 mmol) and cyclopropylacetic acid (36 mg, 0.36 mmol). Purification by flash column chromatography (SiO_2, DCM/EtOH 96:04) afforded **1l** as a yellow solid (53 mg, 58 %). ^{1}H NMR (300 MHz, DMSO-d_6) δ 0.11 - 0.23 (m, 2H), 0.40 - 0.51 (m, 2H), 0.93 - 1.13 (m, 1H), 2.26 (d, *J* = 7.1 Hz, 2H), 2.63 (s, 3H), 7.03 (dd, *J* = 5.4, 1.6 Hz, 1H), 7.26 (t, *J* = 8.9 Hz, 2H), 7.50 (dd, *J* = 8.9, 5.5 Hz, 2H), 8.16 (d, *J* = 5.4 Hz, 1H), 8.23 (d, *J* = 0.64 Hz, 1H), 10.44 (s, 1H). ^{13}C NMR (75 MHz, DMSO-d_6) δ 4.0, 7.6, 15.0, 41.0, 110.6, 115.7 (d, $^{2}J_{CF}$ = 21.6 Hz), 116.6, 130.5 (d, $^{3}J_{CF}$ = 7.8 Hz), 142.9, 146.8, 152.0, 161.9 (d, $^{1}J_{CF}$ = 245.4 Hz), 171.8. TLC-MS (ESI) *m/z* = 383.0 $[M + H]^+$ *m/z* = 381.0 $[M - H]^-$. HPLC: t_R = 6.04 min (100.0 % purity).

*4.2.5.20. N-(4-(5-(4-Fluorophenyl)-2-(methylthio)-1H-imidazol-4-yl)pyridin-2-yl)cyclobutanecarboxamide (**1m**)*

Compound **10a** (125 mg, 0.30 mmol) was dissolved in pyridine (5 mL) and cooled to 0 °C. Cyclobutanecarbonyl chloride (102 µL, 0.89 mmol) was added dropwise with a syringe and the mixture was stirred overnight at rt. Purification by flash column chromatography (SiO_2, *n*-hexane/EtOAc 70:30) afforded **1m** as a yellow solid (24 mg, 21 %). ^{1}H NMR (300 MHz, $CDCl_3$) δ 1.80 - 2.04 (m, 2H), 2.12 - 2.25 (m, 2H), 2.25 - 2.40 (m, 2H), 2.65 (s, 3H), 3.18 (quin, *J* = 8.5 Hz, 1H), 6.97 - 7.07 (m, 3H), 7.43 (dd, *J* = 8.1, 5.6 Hz, 2H), 8.04 (dd, *J* = 5.4, 0.4 Hz, 1H), 8.16 (br. s., 1H), 8.36 (s, 1H); ^{13}C NMR (75 MHz, $CDCl_3$) δ 16.1, 17.9, 25.1, 40.7, 111.0, 115.7 (d, $^{2}J_{CF}$ = 21.6 Hz), 117.6, 130.1 (d, $^{3}J_{CF}$ = 8.3 Hz), 147.4, 151.7, 162.6 (d, $^{1}J_{CF}$ = 248.2 Hz), 173.9; TLC-MS (ESI) *m/z* = 383.2 $[M + H]^+$ *m/z* = 381.2 $[M - H]^-$. HPLC: t_R = 6.30 min (99.1 % purity)

*4.2.5.21. N-(4-(5-(4-Fluorophenyl)-2-(methylthio)-1H-imidazol-4-yl)pyridin-2-yl)-3-oxocyclobutane-1-carboxamide (**1n**)*

The title compound was prepared according to **general procedure B** starting from **10a** (72 mg, 0.24 mmol) and 3-oxocyclobutanecarboxylic acid (41 mg, 0.36 mmol). Purification by flash column chromatography (SiO_2, *n*-hexane/EtOAc 50:50) afforded **1n** as a yellow solid (88 mg, 93 %). ^{1}H NMR (300 MHz, DMSO-d_6) δ 2.62 (s, 3H), 3.25 (td, J = 4.8, 2.3 Hz, 4H), 3.40 - 3.55 (m, 1H), 7.01 (dd, J = 5.3, 1.6 Hz, 1H), 7.25 (t, J = 8.9 Hz, 2H), 7.44 - 7.54 (m, 2H), 8.17 (d, J = 5.2 Hz, 1H), 8.36 (s, 1H), 10.71 (s, 1H). ^{13}C NMR (75 MHz, DMSO-d_6) δ 15.1, 28.1, 51.0, 110.8, 115.7 (d, $^2J_{CF}$ = 21.6 Hz), 116.8, 130.4 (d, $^3J_{CF}$ = 8.3 Hz), 142.7, 147.8, 152.4, 161.8 (d, $^1J_{CF}$ = 244.9 Hz), 172.9, 205.1. TLC-MS (ESI) m/z = 397.0 $[M + H]^+$ m/z = 395.0 $[M - H]^-$. HPLC: t_R = 4.09 min (97.2 % purity).

*4.2.5.22. trans-3-Chloro-N-(4-(5-(4-fluorophenyl)-2-(methylthio)-1H-imidazol-4-yl)pyridin-2-yl)cyclobutane-1-carboxamide (**1o**) and cis-3-hloro-N-(4-(5-(4-fluorophenyl)-2-(methylthio)-1H-imidazol-4-yl)pyridin-2-yl)cyclobutane-1-carboxamide (**1p**)*

The title compounds were prepared according to **general procedure C** starting from **10a** (72 mg, 0.24 mmol) and 3-chlorocyclobutanecarboxylic acid (48 mg, 0.36 mmol). Purification by flash column chromatography (SiO_2, DCM/EtOH 97:03) afforded the separated cis and trans isomers each as a yellow solid (total yield 85 mg, 85 % in a ratio of trans/cis 2.5:1). The *cis* and *trans* geometry was confirmed by 2D NOESY experiments.

trans-3-Chloro-_N_-(4-(5-(4-fluorophenyl)-2-(methylthio)-1_H_-imidazol-4-yl)pyridin-2-yl)cyclobutane-1-carboxamide (1o)

^{1}H NMR (300 MHz, DMSO-d_6) δ 2.37 - 2.48 (m, 2H), 2.62 (s, 3H), 2.75 (ddd, J = 13.07, 7.75, 4.9 Hz, 2H), 3.56 (tt, J = 9.5, 4.8 Hz, 1H), 4.65 (quin, J = 6.8 Hz, 1H), 6.99 (dd, J = 5.3, 1.5 Hz, 1H), 7.27 (br. s., 2H), 7.48 (dd, J = 8.6, 5.6 Hz, 2H), 8.13 (br. s., 1H), 8.36 (br. s., 1H), 10.39 (br. s., 1H), 12.72 (br. s., 1H). ^{13}C NMR (75 MHz, MeOD) δ 16.8, 37.6, 38.3, 52.5, 113.4, 116.9 (d, $^2J_{CF}$ = 21.6 Hz), 119.0, 131.8 (d, $^3J_{CF}$ = 8.3 Hz), 145.2, 149.2, 153.6,

164.3 (d, $^{1}J_{CF}$ = 247.1 Hz), 175.4. TLC-MS (ESI) *m*/*z* = 417.1 $[M + H]^+$ *m*/*z* = 415.2 $[M - H]^-$ .HPLC: t_R = 6.87 min (98.2 % purity)

cis-3-Chloro-_N_-(4-(5-(4-fluorophenyl)-2-(methylthio)-1_H_-imidazol-4-yl)pyridin-2-yl)cyclobutane-1-carboxamide (1p)

^{1}H NMR (300 MHz, MeOD) δ 2.44 - 2.58 (m, 2H), 2.64 (s, 3H), 2.67 - 2.80 (m, 2H), 2.99 - 3.13 (m, 1H), 4.34 - 4.46 (m, 1H), 7.07 (dd, *J* = 5.3, 1.4 Hz, 1H), 7.13 (t, *J* = 8.8 Hz, 2H), 7.40 - 7.48 (m, 2H), 8.13 (d, *J* = 5.3 Hz, 1H), 8.17 (s, 1H). ^{13}C NMR (75 MHz, MeOD) δ 16.8, 35.9, 38.7, 49.3, 113.4, 116.9 (d, $^{2}J_{CF}$ = 22.1 Hz), 119.1, 131.8 (d, $^{3}J_{CF}$ = 8.3 Hz), 145.3, 149.2, 153.4, 164.3 (d, $^{1}J_{CF}$ = 246.6 Hz), 173.8. TLC-MS (ESI) *m*/*z* = 417.1 $[M + H]^+$ *m*/*z* = 415.2 $[M - H]^-$. HPLC: t_R = 6.64 min (99.1 % purity)

*4.2.5.23. N-(4-(5-(4-Fluorophenyl)-2-(methylthio)-1H-imidazol-4-yl)pyridin-2-yl)-3-oxocyclopentane-1-carboxamide (**1q**)*

The title compound was prepared according to **general procedure C** starting from **10a** (72 mg, 0.24 mmol) and 3-oxocyclopentanecarboxylic acid (53 mg, 0.42 mmol). Purification by flash column chromatography (SiO_2, DCM/EtOH 97:03) afforded **1q** as a yellow solid (53 mg, 54 %). ^{1}H NMR (300 MHz, $CDCl_3$) δ 2.09 - 2.30 (m, 3H), 2.33 - 2.38 (m, 1H), 2.40 - 2.46 (m, 1H), 2.49 - 2.57 (m, 1H), 2.61 (s, 3H), 2.97 - 3.13 (m, 1H), 6.94 - 7.06 (m, 3H), 7.37 (dd, *J* = 8.7, 5.3 Hz, 2H), 7.99 (d, *J* = 5.4 Hz, 1H), 8.24 (br. s., 1H), 8.52 (br. s., 1H). ^{13}C NMR (75 MHz, DMSO-d_6) δ 16.1, 25.3, 27.1, 37.4, 41.4, 111.3, 115.8 (d, $^{2}J_{CF}$ = 22.1 Hz), 117.6, 130.2 (d, $^{3}J_{CF}$ = 7.8 Hz), 143.9, 146.7, 151.5, 162.6 (d, $^{1}J_{CF}$ = 248.2 Hz), 172.9, 217.2. TLC-MS (ESI) *m*/*z* = 433.2 $[M + Na]^+$ *m*/*z* = 409.3 $[M - H]^-$. HPLC: t_R = 4.31 min (98.3 % purity).

*4.2.5.24. N-(4-(5-(4-Fluorophenyl)-2-(methylthio)-1H-imidazol-4-yl)pyridin-2-yl)tetrahydrofuran-2-carboxamide (**1r**)*

The title compound was prepared according to **general procedure B** starting from **10a** (93 mg, 0.30 mmol) and tetrahydro-2-furoic acid (46 mg, 0.40 mmol). Purification by flash

column chromatography (SiO_2, DCM/EtOH 97:03) afforded **1r** as a yellow solid (60 mg, 50 %). ^{1}H NMR (300 MHz, $CDCl_3$) δ 1.79 - 1.97 (m, 2H), 1.99 - 2.11 (m, 1H), 2.19 - 2.34 (m, 1H), 2.60 (s, 3H), 3.85 - 3.95 (m, 1H), 4.01 (dt, *J* = 8.2, 6.5 Hz, 1H), 4.39 (dd, *J* = 8.5, 5.8 Hz, 1H), 6.92 - 7.00 (m, 2H), 7.03 (dd, *J* = 5.4, 1.5 Hz, 1H), 7.33 - 7.41 (m, 2H), 8.07 (dd, *J* = 5.3, 0.6 Hz, 1H), 8.28 - 8.34 (m, 1H), 9.00 (s, 1H). ^{13}C NMR (75 MHz, $CDCl_3$) δ 16.1, 25.5, 30.2, 69.7, 78.3, 110.9, 115.6 (d, $^2J_{CF}$ = 21.6 Hz), 117.9, 130.1 (d, $^3J_{CF}$ = 8.3 Hz), 143.6, 147.8, 150.8, 162.4 (d, $^1J_{CF}$ = 248.1 Hz), 172.3. TLC-MS (ESI) *m*/*z* = 399.2 $[M + H]^+$ *m*/*z* = 397.2 $[M - H]^-$. HPLC: t_R = 5.98 min (97.6 % purity).

*4.2.5.25. N-(4-(5-(4-Fluorophenyl)-2-(methylthio)-1H-imidazol-4-yl)pyridin-2-yl)furan-3-carboxamide (**1t**)*

The title compound was prepared according to **general procedure C** starting from **10a** (72 mg, 0.24 mmol) and 3-furoic acid (37 mg, 0.33 mmol). Purification by flash column chromatography (SiO_2, *n*-hexane/EtOAc 50:50) afforded **1t** as a yellow solid (26 mg, 27 %). ^{1}H NMR (300 MHz, DMSO-d_6) δ 2.68 (s, 3H), 7.10 (dd, *J* = 1.9, 0.7 Hz, 1H), 7.13 (dd, *J* = 5.3, 1.5 Hz, 1H), 7.32 (t, *J* = 8.6 Hz, 2H), 7.52 - 7.61 (m, 2H), 7.82 (t, *J* = 1.7 Hz, 1H), 8.28 (d, *J* = 5.2 Hz, 1H), 8.41 (s, 1H), 8.57 (dd, *J* = 1.4, 0.7 Hz, 1H), 10.61 (s, 1H), 12.76 (br. s., 1H). ^{13}C NMR (75 MHz, DMSO-d_6) δ 15.0, 109.4, 111.6, 115.7 (d, $^2J_{CF}$ = 22.1 Hz), 117.0, 122.5, 130.4 (d, $^3J_{CF}$ = 8.3 Hz), 142.8, 144.3, 146.6, 147.6, 152.3, 160.7, 161.8 (d, $^1J_{CF}$ = 244.9 Hz). TLC-MS (ESI) *m*/*z* = 395.3 $[M + H]^+$ *m*/*z* = 393.2 $[M - H]^-$. HPLC: t_R = 5.90 min (99.3 % purity).

*4.2.5.26. N-(4-(5-(4-Fluorophenyl)-2-(methylthio)-1H-imidazol-4-yl)pyridin-2-yl)picolinamide (**1u**)*

The title compound was prepared according to **general procedure B** starting from **10a** (72 mg, 0.24 mmol) and 3-picolinic acid (44 mg, 0.36 mmol). Purification by flash column chromatography (SiO_2, *n*-hexane/EtOAc 50:50) afforded **1u** as a yellow solid (58 mg, 64 %). ^{1}H NMR (300 MHz, DMSO-d_6) δ 2.65 (s, 3H), 7.15 (dd, *J* = 5.2, 1.6 Hz, 1H), 7.21 -

7.38 (m, 2H), 7.49 - 7.59 (m, 2H), 7.72 (ddd, *J* = 7.5, 4.8, 1.3 Hz, 1H), 8.06 - 8.14 (m, 1H), 8.16 - 8.21 (m, 1H), 8.23 (br. s., 1H), 8.54 (br. s., 1H), 8.75 (dd, *J* = 4.7, 0.5 Hz, 1H), 10.37 (br. s., 1H), 12.77 (br. s., 1H). ^{13}C NMR (75 MHz, DMSO-d_6) δ 15.1, 110.0, 115.9 (d, $^{2}J_{CF}$ = 21.6 Hz), 117.2, 122.2, 126.6 (d, $^{4}J_{CF}$ = 3.3 Hz), 127.5, 130.5, 130.8 (d, $^{3}J_{CF}$ = 8.3 Hz), 134.1, 138.5, 142.4, 144.3, 148.2, 148.5, 148.7, 151.0, 162.1, 161.7 (d, $^{1}J_{CF}$ = 246.6 Hz). TLC-MS (ESI) *m*/*z* = 406.0 $[M + H]^+$ *m*/*z* = 404.0 $[M - H]^-$. HPLC: t_R = 7.71 min (97.5 % purity).

*4.2.5.27. N-(4-(5-(4-Fluorophenyl)-2-(methylthio)-1H-imidazol-4-yl)pyridin-2-yl)-2-(2-oxopyrrolidin-1-yl)acetamide (**1s**)*

The title compound was prepared according to **general procedure A** starting from **11a** (130 mg, 0.41 mmol) and 2-oxopyrrolidin-1-acetamid (87 mg, 0.61 mmol). Purification by flash column chromatography (SiO_2, *n*-hexane/EtOAc 70:30 to 20:80) afforded **1c** as a yellow solid (33 mg, 19 %). ^{1}H NMR (300 MHz, $CDCl_3$) δ 2.01 - 2.17 (m, 2H), 2.42 - 2.53 (m, 2H), 2.64 (s, 3H), 3.51 (t, *J* = 7.0 Hz, 2H), 4.12 (s, 2H), 6.87 - 7.02 (m, 3H), 7.35 (dd, *J* = 8.6, 5.4 Hz, 2H), 7.96 (d, *J* = 5.3 Hz, 1H), 8.12 (br. s., 1H), 9.38 (br. s., 1H). ^{13}C NMR (75 MHz, $CDCl_3$) δ 16.1, 18.0, 30.4, 47.1, 48.5, 111.4, 115.5 (d, $^{2}J_{CF}$ = 21.6 Hz), 117.9, 130.1 (d, $^{3}J_{CF}$ = 8.3 Hz), 143.9, 147.3, 151.3, 162.4 (d, $^{1}J_{CF}$ = 248.7 Hz), 166.6, 176.8. TLC-MS (ESI) *m*/*z* = 447.2 $[M + Na]^+$ *m*/*z* = 423.9 $[M - H]^-$. HPLC: t_R = 3.96 min (100.0 % purity)

4.2.5.36. trans-N-(4-(5-(4-Fluorophenyl)-2-(methylthio)-1H-imidazol-4-yl)pyridin-2-yl)-2-

4.2.5.28. N-(4-(2-(Benzylthio)-5-(4-fluorophenyl)-1*H*-imidazol-4-yl)pyridin-2-yl)-3-(3,4,5-trimethoxyphenyl)propanamide (**2a**)

The title compound was prepared according to **general procedure B** starting from **10b** (78 mg, 0.21 mmol) and 3-(3,4,5-trimethoxyphenyl)propionic acid (65 mg, 0.27 mmol). Purification by flash column chromatography (SiO_2, DCM/EtOH 97:03) afforded **2a** as a yellow solid (56 mg, 45 %). ^{1}H NMR (300 MHz, $CDCl_3$) δ 2.58 - 2.70 (m, 2H), 2.86 - 2.98 (m, 2H), 3.76 (s, 6H), 3.79 (s, 3H), 4.30 (s, 2H), 6.38 (s, 2H), 7.00 (t, *J* = 8.7 Hz, 3H), 7.17

- 7.30 (m, 5H), 7.31 - 7.45 (m, 2H), 7.98 (d, *J* = 5.2 Hz, 1H), 8.32 (br. s., 1H), 8.66 (br. s., 1H). ^{13}C NMR (75 MHz, $CDCl_3$) δ 31.7, 39.0, 39.4, 56.1, 60.8, 105.3, 111.4, 115.7 (d, $^2J_{CF}$ = 21.0 Hz), 117.7, 127.6, 128.7, 129.0, 130.2 (d, $^3J_{CF}$ = 8.3 Hz), 136.2, 136.4, 137.4, 141.1, 147.5, 151.7, 153.2, 162.6 (d, $^1J_{CF}$ = 248.7 Hz), 170.9. TLC-MS (ESI) *m*/*z* = 597.1 $[M - H]^-$. HPLC: t_R = 8.57 min (97.2 % purity).

*4.2.5.29. N-(4-(2-(Benzylthio)-5-(4-fluorophenyl)-1H-imidazol-4-yl)pyridin-2-yl)acetamide (**2b**)*

The title compound was prepared according to **general procedure A** starting from **11b** (100 mg, 0.25 mmol) and acetamide (44 mg, 0.75 mmol). Purification by flash column chromatography (SiO_2, DCM/EtOH 97:03 to 95:05) afforded **2b** as a yellow solid (82 mg, 78 %). ^{1}H NMR (300 MHz, $CDCl_3$) δ 2.08 (s, 3H), 4.28 (s, 2H), 6.93 - 7.03 (m, 2H), 7.08 (br. s., 1H), 7.18 - 7.28 (m, 5 H), 7.35 (br. s., 2H), 8.01 (d, *J* = 5.3 Hz, 1H), 8.30 (br. s., 1H), 9.11 (br. s., 1H), 10.67 (br. s., 1H). ^{13}C NMR (75 MHz, $CDCl_3$) δ 24.4, 38.9, 111.4, 115.7 (d, *J* = 21.7 Hz), 117.7, 127.5, 128.5, 128.9, 130.1 (d, *J* = 8.3 Hz), 137.3, 141.3, 147.3, 151.8, 162.5 (d, *J* = 248.3 Hz), 169.2. TLC-MS (ESI) *m*/*z* = 419.2 $[M + H]^+$ *m*/*z* = 417.0 $[M - H]^-$. HPLC: t_R = 6.42 min (98.2 % purity)

*4.2.5.30. N-(4-(2-(Benzylthio)-5-(4-fluorophenyl)-1H-imidazol-4-yl)pyridin-2-yl)cyclopropanecarboxamide (**2c**)*

The title compound was prepared according to **general procedure A** starting from **11b** (125 mg, 0.32 mmol) and cyclopropanecarboxamide (40 mg, 0.47 mmol). Purification by flash column chromatography (SiO_2, DCM/EtOH 97:03 to 95:05) afforded **2c** as a yellow solid (90 mg, 64 %). ^{1}H NMR (300 MHz, $CDCl_3$) δ 0.77 - 0.89 (m, 2H), 0.98 - 1.07 (m, 2H), 1.47 - 1.62 (m, 1H), 4.28 (s, 2H), 6.99 (t, *J* = 8.6 Hz, 3H), 7.15 - 7.29 (m, 5 H), 7.35 (br. s., 2H), 8.02 (d, *J* = 5.3 Hz, 1H), 8.26 (br. s., 1H), 9.10 (br. s., 1H). ^{13}C NMR (75 MHz, $CDCl_3$) δ 8.4, 15.7, 39.0, 111.4, 115.7 (d, $^2J_{CF}$ = 22.2 Hz), 117.4, 127.5, 128.6, 129.0, 130.1 (d,

$^{3}J_{CF}$ = 8.3 Hz), 137.3, 141.0, 147.3, 151.9, 162.5 (d, $^{1}J_{CF}$ = 247.9 Hz), 172.6. TLC-MS (ESI) *m*/*z* = 445.6 $[M + H]^+$ *m*/*z* = 443.3 $[M - H]^-$. HPLC: t_R = 7.62 min (98.9 % purity).

*4.2.5.31. N-(4-(2-(Benzylthio)-5-(4-fluorophenyl)-1H-imidazol-4-yl)pyridin-2-yl)cyclopentanecarboxamide (**2d**)*

The title compound was prepared according to **general procedure B** starting from **10b** (78 mg, 0.21 mmol) and cyclopentanecarboxylic acid (31 mg, 0.27 mmol). Purification by flash column chromatography (SiO_2, *n*-hexane/EtOAc 70:30 to 0:100) afforded **2d** as a yellow solid (40 mg, 41 %). ^{1}H NMR (300 MHz, $CDCl_3$) δ 1.52 - 1.98 (m, 8H), 2.71 (quin, *J* = 7.9 Hz, 1H), 4.29 (s, 2H), 6.93 - 7.06 (m, 3H), 7.19 - 7.30 (m, 5H), 7.31 - 7.45 (m, 2H), 8.00 (d, *J* = 5.4 Hz, 1H), 8.34 (br. s., 1H), 8.66 (br. s., 1H). ^{13}C NMR (75 MHz, $CDCl_3$) δ 26.0, 30.4, 39.0, 46.7, 111.4, 115.8 (d, $^{2}J_{CF}$ = 21.5 Hz), 117.5, 127.6, 128.6, 129.0, 130.2 (d, $^{3}J_{CF}$ = 8.3 Hz), 137.4, 141.0 ,147.1, 152.0, 162.6 (d, $^{1}J_{CF}$ = 248.4 Hz), 175.4. TLC-MS (ESI) *m*/*z* = 472.9 $[M + H]^+$ *m*/*z* = 471.1 $[M - H]^-$. HPLC: t_R = 9.14 min (95.4 % purity).

4.2.5.32. N-(4-(2-(Benzylthio)-5-(4-fluorophenyl)-1*H*-imidazol-4-yl)pyridin-2-yl)-2-(4-fluorophenyl)acetamide (**2e**)

The title compound was prepared according to **general procedure B** starting from **10b** (78 mg, 0.21 mmol) and 4-fluorophenylacetic acid (42 mg, 0.27 mmol). Purification by flash column chromatography (SiO_2, DCM/EtOH 97:03 to 95:05) afforded **2e** as a yellow solid (73 mg, 69 %). ^{1}H NMR (300 MHz, $CDCl_3$) δ 3.67 (s, 2H), 4.30 (s, 2H), 6.96 - 7.11 (m, 5H), 7.18 - 7.32 (m, 7H), 7.37 (br. s., 2H), 8.02 (d, *J* = 5.4 Hz, 1H), 8.17 (br. s., 1H), 8.28 (br. s., 1H). ^{13}C NMR (75 MHz, $CDCl_3$) δ 38.8, 43.7, 111.1, 115.8 (d, $^{2}J_{CF}$ = 21.6 Hz), 115.9 (d, $^{2}J_{CF}$ = 21.0 Hz), 117.8, 127.5, 128.6, 129.0, 129.5 (d, $^{4}J_{CF}$ = 3.3 Hz), 130.1 (d, $^{3}J_{CF}$ = 7.7 Hz), 130.9 (d, $^{3}J_{CF}$ = 8.3 Hz), 137.4, 141.3, 147.4, 151.4, 162.1 (d, $^{1}J_{CF}$ = 246.6 Hz), 162.6 (d, $^{1}J_{CF}$ = 248.2 Hz), 169.6. TLC-MS (ESI) *m*/*z* = 534.9 $[M + Na]^+$ *m*/*z* = 511.2 $[M - H]^-$. HPLC: t_R = 10.54 min (95.0 % purity).

*4.2.5.33. N-(4-(4-(4-Fluorophenyl)-2-(methylsulfinyl)-1H-imidazol-5-yl)pyridin-2-yl)cyclopropanecarboxamide (**12a**)*

Compound **1c** (73 mg, 0.19 mmol) was dissolved in acetontrile (10 ml) and a 28-31 % wt. aqueous solution of H_2O_2 (20 µL, 0.195 mmol) was added before the solution was stirred for 24 h at rt. An additional 60 µL (0.585 mmol) of aqueous H_2O_2 solution (0.39 mmol) was added and the mixture was further stirred until reaction control by TLC showed complete conversion of the starting material (48 h). Purification by flash column chromatography (SiO_2, DCM/EtOH 97:3) afforded **12a** as a yellow solid (37 mg, 51 %). ^{1}H NMR (300 MHz, $CDCl_3$) δ 0.82 - 0.92 (m, 2H), 1.02 - 1.12 (m, 2H), 1.61 - 1.74 (m, 1H), 3.12 (s, 3H), 6.94 (d, *J* = 4.8 Hz, 1H), 7.08 (t, *J* = 8.6 Hz, 2H), 7.39 - 7.49 (m, 2H), 7.88 (d, *J* = 5.3 Hz, 1H), 8.50 (s, 1H), 9.30 (br. s., 1H), 13.08 (br. s, 1H). ^{13}C NMR (75 MHz, $CDCl_3$) δ 8.5, 15.6, 40.9, 112.1, 116.0 (d, $^2J_{CF}$ = 21.0 Hz), 117.4, 130.7 (d, $^3J_{CF}$ = 8.3 Hz), 146.9, 147.9, 152.2, 163.0 (d, $^1J_{CF}$ = 247.1 Hz), 172.7; TLC-MS (ESI) *m*/*z* = 407.2 $[M + Na]^+$ *m*/*z* = 383.2 $[M - H]^-$. HPLC: t_R = 3.47 min (100.0 % purity).

*4.2.5.34. N-(4-(4-(4-Fluorophenyl)-2-(methylsulfinyl)-1H-imidazol-5-yl)pyridin-2-yl)cyclobutanecarboxamide (**12b**)*

Compound **1m** (60 mg, 0.16 mmol) was dissolved in acetonitrile (10 ml) and a 28-31 % wt. aqueous solution of H_2O_2 (30 µL, 0.293 mmol) was added before the solution was stirred for 24 h at rt. An additional 60 µL (0.585 mmol) of aqueous H_2O_2 solution (0.39 mmol) was added and the mixture was further stirred until reaction control by TLC showed complete conversion of the starting material (72 h). Purification by flash column chromatography (SiO2, *n*-hexane/EtOAc 70:30 to 20:80) afforded **12b** as a yellow solid (26 mg, 42 %). ^{1}H NMR (300 MHz, DMSO-d_6) δ 1.72 - 1.85 (m, 1H), 1.85 - 2.00 (m, 1H), 2.01 - 2.26 (m, 4H), 3.09 (s, 3H), 3.35 (quin, *J* = 8.2 Hz, 1H), 6.99 (dd, *J* = 5.2, 1.5 Hz, 1H), 7.29 (t, *J* = 8.9 Hz, 2H), 7.47 - 7.58 (m, 2H), 8.18 (d, *J* = 5.2 Hz, 1H), 8.38 (s, 1H), 10.27 (s, 1H), 13.89 (br. s., 1H). ^{13}C NMR (75 MHz, DMSO-d_6) δ 17.7, 24.4, 39.1, 111.2, 115.8 (d, $^2J_{CF}$ = 21.6 Hz),

116.9, 130.8 (d, $^{3}J_{CF}$ = 8.3 Hz), 147.9, 148.8, 152.7, 162.1 (d, $^{1}J_{CF}$ = 244.9 Hz), 173.6. TLC-MS (ESI) *m*/*z* = 421.1 $[M + Na]^+$ *m*/*z* = 397.2 $[M - H]^-$. HPLC: t_R = 4.81 min (99.8 % purity).

*4.2.5.35. N-(4-(4-(4-Fluorophenyl)-1-methyl-2-(methylthio)-1H-imidazol-5-yl)pyridin-2-yl)cyclopropanecarboxamide (**14**)*[25]

4-(4-(4-Fluorophenyl)-1-methyl-2-(methylthio)-1*H*-imidazol-5-yl)pyridin-2-amine (**13**)[25] (150 mg, 0.48 mmol) was dissolved in pyridine (5 mL) and cooled to 0 °C. Cyclopropanecarbonyl chloride (87 µL, 0.95 mmol) was added dropwise via syringe. The reaction was stirred for 2 h before H_2O (40 mL) was added and it was extracted with ethyl acetate (3x). The combined organic layers were dried over anhydrous Na_2SO_4, concentrated in vacuo and purified by flash column chromatography (SiO_2, n-hexane/EtOAc 50:50) to give **14** as a yellow solid (57 mg, 31 %). ^{1}H NMR (300 MHz, DMSO-d_6) δ 0.79 - 0.90 (m, 4H), 2.01 - 2.12 (m, 1H), 2.69 (s, 3H), 3.44 (s, 3H), 7.06 - 7.22 (m, 3H), 7.39 - 7.53 (m, 2H), 8.10 (d, *J* = 0.5 Hz, 1H), 8.46 (dd, *J* = 5.0, = 0.6 Hz, 1H), 11.02 (s, 1H). ^{13}C NMR (75 MHz, DMSO-d_6) δ 7.7, 14.2, 15.3, 31.6, 114.3, 115.2 (d, $^{2}J_{CF}$ = 21.0 Hz), 120.3, 127.9, 128.2 (d, $^{3}J_{CF}$ = 7.7 Hz), 130.4 (d, $^{4}J_{CF}$ = 3.3 Hz), 137.0, 139.9, 143.9, 148.8, 152.8, 161.0 (d, $^{1}J_{CF}$ = 245.5 Hz), 172.8; TLC-MS (ESI) *m*/*z* = 383.1 $[M + H]^+$ *m*/*z* = 383.1 $[M - H]^-$. HPLC: t_R = 6.39 min (100.0 % purity).

*4.2.5.36. N-(4-(5-(4-Fluorophenyl)-1-methyl-2-(methylthio)-1H-imidazol-4-yl)pyridin-2-yl)cyclopropanecarboxamide (**16**)*

The title compound was prepared according to **general procedure A** starting from 2-chloro-4-(5-(4-fluorophenyl)-1-methyl-2-(methylthio)-1*H*-imidazol-4-yl)pyridine (**15**)[22] (100 mg, 0.30 mmol) and cyclopropanecarboxamide (38.3 mg, 0.45 mmol). Purification by flash column chromatography (SiO_2, *n*-hexane/EtOAc 70:30 to 50:50) afforded **16** as a yellow solid (72 mg, 63 %). ^{1}H NMR (300 MHz, $CDCl_3$) δ 0.77 - 0.86 (m, 2H), 1.01 - 1.09 (m, 2H), 1.46 - 1.58 (m, 1H), 2.73 (s, 3H), 3.35 (s, 3H), 6.96 (dd, *J* = 5.3, 1.6 Hz, 1H), 7.15

- 7.23 (m, 2H), 7.27 - 7.34 (m, 2H), 8.01 (dd, *J* = 5.4, 0.6 Hz, 1H), 8.33 (s, 1H), 8.85 (br. s, 1H). ^{13}C NMR (75 MHz, $CDCl_3$) 8.1, 15.5, 15.7, 31.2, 111.0, 116.5 (d, $^2J_{CF}$ = 21.6 Hz), 119.2, 125.9 (d, $^4J_{CF}$ = 3.3 Hz), 132.0 (d, $^3J_{CF}$ = 8.3 Hz), 132.4, 135.8, 144.3, 144.3, 147.0, 151.9, 163.2 (d, $^1J_{CF}$ = 249.9 Hz), 171.9; TLC-MS (ESI) *m*/*z* = 383.4 $[M + H]^+$ *m*/*z* = 381.4 $[M - H]^-$. HPLC: t_R = 5.50 min (98.9 % purity).

*4.2.5.37. 1-(4-Fluorophenyl)-2-(2-((4-methoxybenzyl)amino)pyridin-4-yl)ethane-1,2-dione (**17**)*

Compound **7** (4.00 g, 8.88 mmol) was dissolved in acetic acid and selenium dioxide (1.17 g, 10.66 mmol) was added. The reaction mixture was stirred at 130 °C for 1.5 h. After cooling to rt, the mixture was filtered and the solvent was removed under reduced pressure. The residue was dissolved in DCM (20 mL) and washed with sat. sodium bicarbonate solution (3x). The aqueous layer was adjusted to pH 10-11 with 1 M NaOH and extracted twice with DCM. The combined organic layers were dried over anhydrous Na_2SO_4 and the compound was purified by flash chromatography (SiO_2, *n*-hexane/EtOAc 85:15 to 70:30) to give **17** as a yellow solid (1.41 g, 44 %). ^{1}H NMR (300 MHz, $CDCl_3$) δ 3.80 (s, 3H), 4.47 (d, *J* = 4.3 Hz, 2H), 5.20 (br. s., 1H), 6.81 - 6.89 (m, 3H), 7.00 (dd, *J* = 5.3, 1.4 Hz, 1H), 7.14 - 7.27 (m, 4H), 7.93 - 8.01 (m, 2H), 8.29 (dd, *J* = 5.2, 0.7 Hz, 1H). TLC-MS (ESI) *m*/*z* = 397.1 $[M + MeOH]^+$ *m*/*z* = 363.0 $[M - H]^-$. HPLC: t_R = 5.40 min.

*4.2.5.38. 1-(2-Aminopyridin-4-yl)-2-(4-fluorophenyl)ethane-1,2-dione (**18**)*

Compound **17** (1.18 g, 3.25 mmol) was dissolved in TFA (15 mL) and stirred at rt until reaction control by TLC showed complete conversion. The solvent was removed under reduced pressure and the residue was dissolved in DCM (20 mL) and washed with sat. sodium bicarbonate solution (3x). The aqueous layer was adjusted to pH 10-11 with 1 M NaOH and extracted twice with DCM. The combined organic layers were dried over anhydrous Na_2SO_4 and purified by flash chromatography (SiO_2, *n*-hexane/EtOAc 70:30 to

50:50) to give **18** as an orange-yellow solid (769 mg, 97 %). ^{1}H NMR (300 MHz, $CDCl_3$) δ 6.46 (s, 2H), 6.84 - 6.87 (m, 2H), 7.47 (t, *J* = 8.9 Hz, 2H), 8.03 (dd, *J* = 9.0, 5.4 Hz, 2H), 8.17 (d, *J* = 6.1 Hz, 1H). ^{13}C NMR (75 MHz, DMSO-d_6) δ 107.8, 108.7, 116.9 (d, $^{2}J_{CF}$ = 22.1 Hz), 128.7 (d, $^{4}J_{CF}$ = 2.8 Hz), 133.0 (d, $^{3}J_{CF}$ = 10.5 Hz), 139.3, 149.8, 160.7, 166.4 (d, $^{1}J_{CF}$ = 256.5 Hz), 192.4, 194.6. TLC-MS (ESI) *m*/*z* = 276.9 $[M + MeOH]^+$ *m*/*z* = 242.9 $[M - H]^-$. HPLC: t_R = 2.18 min.

*4.2.5.39. N-(Cyclopropanecarbonyl)-N-(4-(2-(4-fluorophenyl)-2-oxoacetyl)pyridin-2-yl)cyclopropanecarboxamide (**19b**)*

Compound **18** (1.06 g, 4.35 mmol) was dissolved in DCM (15 mL), cooled to 0 °C and *N*,*N*-diisopropylethylamine (2.50 mL, 15.22 mmol) was added. Subsequently a solution of cyclopropanecarbonyl chloride (1.82 g, 17.39 mmol) in DCM (10 mL) was added dropwise to the cooled solution. After 1 h, the cooling bath was removed and the mixture was stirred at rt for 17 h. Water (50 mL) was added and the organic layer was collected, washed with sat. sodium bicarbonate solution (2x) and dried over anhydrous Na_2SO_4. Purification by flash chromatography (SiO_2, *n*-hexane/EtOAc 90:10 to 50:50) afforded **19b** as an orange solid (350 mg, 21 %). ^{1}H NMR (300 MHz, $CDCl_3$) δ 0.91 - 0.99 (m, 4H), 1.17 - 1.24 (m, 4H), 1.99 (tt, *J* = 7.9, 4.6 Hz, 2H), 7.19 - 7.26 (m, 2H), 7.79 - 7.86 (m, 2H), 8.01 - 8.14 (m, 2H), 8.85 (dd, *J* = 5.0, 0.9 Hz, 1H). TLC-MS (ESI) *m*/*z* = 435.0 $[M + MeOH + Na]^+$. HPLC: t_R = 6.89 min.

*4.2.5.40. N-(4-(4-(4-Fluorophenyl)-1H-imidazol-5-yl)pyridin-2-yl)cyclopropanecarboxamide (**20a**)*

The title compound was prepared according to **general procedure D** starting from **19b** (200 mg, 0.53 mmol) using ammonium acetate (811 mg, 10.52 mmol) and paraformaldehyde (24 mg, 0.79 mmol). Purification by flash chromatography (SiO_2, DCM/EtOH 95:05) afforded **20a** as a white solid (110 mg, 65 %). ^{1}H NMR (300 MHz, DMSO-d_6) δ 0.78 (d, *J* = 5.9 Hz, 4H), 1.95 - 2.04 (m, 1H), 7.01 (dd, *J* = 5.2, 1.5 Hz, 1H),

7.26 (t, *J* = 8.9 Hz, 2H), 7.45 - 7.54 (m, 2H), 7.87 (s, 1H), 8.17 (d, *J* = 5.2 Hz, 1H), 8.33 (s, 1H), 10.73 (s, 1H), 12.79 (br. s., 1H). ^{13}C NMR (75 MHz, DMSO-d_6) δ 7.6, 14.2, 110.9, 115.7 (d, $^{2}J_{CF}$ = 22.1 Hz), 116.7, 130.3 (d, $^{3}J_{CF}$ = 8.3 Hz), 136.4, 147.8, 152.6, 161.7 (d, $^{1}J_{CF}$ = 244.4 Hz), 172.4.TLC-MS (ESI) *m*/*z* = 322.9 $[M + H]^+$ *m*/*z* = 321.0 $[M - H]^-$. HPLC: t_R = 2.98 min (98.3 % purity).

*4.2.5.41. N-(4-(4-(4-Fluorophenyl)-2-methyl-1H-imidazol-5-yl)pyridin-2-yl)cyclopropanecarboxamide (**20b**)*

The title compound was prepared according to **general procedure D** starting from **19b** (100 mg, 0.26 mmol) using ammonium acetate (405 mg, 5.26 mmol) and acetaldehyde (17 mg, 0.39 mmol). Purification by flash chromatography (SiO_2, DCM/EtOH 95:05 to 90:10) afforded **20b** as a white solid (10 mg, 11 %). ^{1}H NMR (300 MHz, DMSO-d_6) δ 0.78 (d, *J* = 6.1 Hz, 4H), 1.94 - 2.03 (m, 1H), 2.34 (s, 3H), 6.96 (dd, *J* = 5.2, 1.6 Hz, 1H), 7.23 (t, *J* = 8.8 Hz, 2H), 7.42 - 7.50 (m, 2H), 8.12 (d, *J* = 5.1 Hz, 1H), 8.29 (br. s., 1H), 10.66 (br. s., 1H), 12.33 (br. s., 1H). ^{13}C NMR (75 MHz, $CDCl_3$) δ 8.4, 13.9, 25.6, 111.0, 115.6 (d, $^{2}J_{CF}$ = 21.6), 117.4, 130.0 (d, $^{3}J_{CF}$ = 8.3 Hz), 145.6, 147.6, 151.9, 162.4 (d, $^{1}J_{CF}$ = 247.7 Hz), 172.7. TLC-MS (ESI) *m*/*z* = 337.1 $[M + H]^+$ *m*/*z* = 335.1 $[M - H]^-$. HPLC: t_R = 3.43 min (95.7 %)

*4.2.5.42. N-(4-(2-Ethyl-4-(4-fluorophenyl)-1H-imidazol-5-yl)pyridin-2-yl)cyclopropanecarboxamide (**20c**)*

The title compound was prepared according to **general procedure D** starting from **19b** (150 mg, 0.39 mmol) using ammonium acetate (608 mg, 7.89 mmol) and propionaldehyde (34 mg, 0.59 mmol). Purification by flash chromatography (SiO_2, DCM/EtOH 97:03 to 94:06) afforded **20c** as a white solid (47 mg, 34 %). ^{1}H NMR (300 MHz, $CDCl_3$) δ 0.81 - 0.89 (m, 2H), 0.99 - 1.05 (m, 2H), 1.29 (t, *J* = 7.7 Hz, 3H), 1.53 - 1.63 (m, 1H), 2.71 (q, *J* = 7.6 Hz, 2H), 6.94 - 7.03 (m, 3H), 7.39 (dd, *J* = 8.6, 5.4 Hz, 2H), 8.05 (d, *J* = 5.4 Hz, 1H), 8.26 (s, 1H), 9.19 (br. s., 1H). ^{13}C NMR (75 MHz, $CDCl_3$) δ 8.4, 12.6, 15.7, 21.7, 111.2,

115.6 (d, $^{2}J_{CF}$ = 21.6 Hz), 117.5, 130.1 (d, $^{3}J_{CF}$ = 8.3 Hz), 147.4, 150.8, 152.0, 162.4 (d, $^{1}J_{CF}$ = 247.1 Hz), 172.7. TLC-MS (ESI) *m*/*z* = 351.0 $[M + H]^{+}$ *m*/*z* = 349.1 $[M - H]^{-}$. HPLC: t_R = 3.84 min (95.1 % purity).

*4.2.5.43. N-(4-(4-(4-Fluorophenyl)-2-phenyl-1H-imidazol-5-yl)pyridin-2-yl)cyclopropanecarboxamide (**20d**)*

The title compound was prepared according to **general procedure D** starting from **19b** (100 mg, 0.26 mmol) using ammonium acetate (405 mg, 5.26 mmol) and benzaldehyde (42 mg, 0.39 mmol). Purification by flash chromatography (SiO_2, *n*-hexane/EtOAc 50:50) afforded **20d** as a white solid (25 mg, 24 %). ^{1}H NMR (300 MHz, DMSO-d_6) δ 0.75 - 0.84 (m, 4H), 1.96 - 2.05 (m, 1H), 7.06 (dd, *J* = 5.3, 1.4 Hz, 1H), 7.29 (t, *J* = 8.5 Hz, 2H), 7.36 - 7.44 (m, 1H), 7.44 - 7.53 (m, 2H), 7.53 - 7.62 (m, 2H), 8.04 - 8.11 (m, 2H), 8.18 (d, *J* = 4.6 Hz, 1H), 8.40 (br. s., 1H), 10.73 (br. s., 1H). ^{13}C NMR (75 MHz, DMSO-d_6) δ 7.6, 14.2, 111.1, 115.7 (d, $^{2}J_{CF}$ = 21.6 Hz), 116.5, 125.4, 128.7, 128.8, 129.9, 130.9 (d, $^{3}J_{CF}$ = 8.9 Hz), 146.2, 147.7, 152.5, 161.9 (d, $^{1}J_{CF}$ = 242.1 Hz), 172.4. TLC-MS (ESI) *m*/*z* = 421.0 $[M + Na]^{+}$ *m*/*z* = 397.0 $[M - H]^{-}$. HPLC: t_R = 6.74 min (98.9 % purity).

*4.2.5.44. N-(4-(2-Benzyl-4-(4-fluorophenyl)-1H-imidazol-5-yl)pyridin-2-yl)cyclopropanecarboxamide (**20e**)*

The title compound was prepared according to **general procedure D** starting from **19b** (150 mg, 0.39 mmol) using ammonium acetate (608 mg, 7.89 mmol) and phenylacetaldehyde (61 mg, 0.59 mmol). Purification by flash chromatography (SiO_2, *n*-hexane/EtOAc 70:30 to 30:70) afforded **20e** as a tan white solid (8 mg, 5 %). ^{1}H NMR (300 MHz, DMSO-d_6) δ 0.82 (d, *J* = 5.96 Hz, 4H), 2.01 - 2.06 (m, 1H), 4.03 - 4.13 (m, 2H), 7.01 (dd, *J* = 5.27, 1.51Hz, 1H), 7.27 (td, *J* = 5.91, 2.48 Hz, 3H), 7.32 - 7.41 (m, 4H), 7.51 (dd, *J* = 8.62, 5.59 Hz, 2H), 8.16 (br. s., 1H), 8.34 (br. s., 1H), 10.72 (br. s., 1H), 12.21 - 12.99 (m, 1H). ^{13}C NMR (75 MHz, DMSO-d_6) δ 7.6, 14.2, 34.0, 110.7, 115.6 (d, $^{2}J_{CF}$ = 22.1 Hz), 116.6, 126.4, 128.4, 128.5, 130.3 (d, $^{3}J_{CF}$ = 7.7 Hz), 138.2, 147.7, 152.6, 161.8 (d, $^{1}J_{CF}$ =

244.9 Hz), 172.4. TLC-MS (ESI) *m*/*z* = 413.1 $[M + H]^+$ *m*/*z* = 411.1 $[M - H]^-$. HPLC: t_R = 6.65 min (95.9 % purity).

*4.2.5.45. N-(4-(4-(4-Fluorophenyl)-2-phenethyl-1H-imidazol-5-yl)pyridin-2-yl)cyclopropanecarboxamide (**20f**)*

Compound **19b** (150 mg, 0.39 mmol) was dissolved in methanol (8 mL) before 7 M ammonia in methanol (1.12 mL, 7.89 mmol) and 3-phenylpropionaldehyde (79 mg, 0.59 mmol) were added. The reaction was heated to 80 °C for 3 h. Evaporation of the solvent and subsequent purification by flash chromatography (SiO_2, *n*-hexane/EtOAc 90:10 to 15:85) afforded **20f** as a brown solid (25 mg, 15 %). ^{1}H NMR (300 MHz, DMSO-d_6) δ 0.79 (d, *J* = 6.1 Hz, 4H), 2.00 (quin, *J* = 6.2 Hz, 1H), 2.91 - 3.10 (m, 4H), 6.98 (dd, *J* = 5.2, 1.6 Hz, 1H), 7.15 - 7.37 (m, 7H), 7.48 (dd, *J* = 8.7, 5.6 Hz, 2H), 8.08 - 8.41 (m, 2H), 10.68 (br. s., 1H), 12.42 (br. s., 1H). ^{13}C NMR (75 MHz, $CDCl_3$) δ 8.5, 15.8, 30.5, 34.7, 111.2, 115.7 (d, $^2J_{CF}$ = 21.6 Hz), 117.5, 126.4, 128.4, 128.6, 130.1 (d, $^3J_{CF}$ = 8.3 Hz), 140.7, 147.5, 148.8, 152.0, 162.5 (d, $^1J_{CF}$ = 247.7 Hz), 172.7. TLC-MS (ESI) *m*/*z* = 427.1 $[M + H]^+$ *m*/*z* = 425.2 $[M - H]^-$. HPLC: t_R = 6.89 min (97.5 % purity).

*4.2.5.46. N-(4-(4-(4-Fluorophenyl)-2-(furan-2-yl)-1H-imidazol-5-yl)pyridin-2-yl)cyclopropanecarboxamide (**20g**)*

The title compound was prepared according to **general procedure D** starting from **19b** (150 mg, 0.39 mmol) using ammonium acetate (608 mg, 7.89 mmol) and 2-furaldehyde (57 mg, 0.59 mmol). Purification by flash chromatography (SiO_2, DCM/EtOH 97:03 to 95:05) afforded **20g** as a brown solid (79 mg, 52 %). ^{1}H NMR (300 MHz, DMSO-d_6) δ 0.80 (d, *J* = 5.9 Hz, 4H), 1.13 - 1.24 (m, 1H), 6.66 (dd, *J* = 3.2, 1.7 Hz, 1H), 7.02 (d, *J* = 3.4 Hz, 2H), 7.29 (br. s., 2H), 7.55 (dd, *J* = 8.6, 5.6 Hz, 2H), 7.84 (s, 1H), 8.12 - 8.44 (m, 2H), 10.76 (br. s., 1H), 13.10 (br. s., 1H). ^{13}C NMR (75 MHz, DMSO-d_6) δ 7.6, 14.2, 108.1, 111.1, 111.9, 115.7 (d, $^2J_{CF}$ = 21.6 Hz), 116.9, 130.7 (d, $^3J_{CF}$ = 8.3 Hz), 139.2, 143.4,

145.2, 147.7, 152.5, 161.9 (d, $^1J_{CF}$ = 245.5 Hz), 172.4. TLC-MS (ESI) *m*/*z* = 389.0 $[M + H]^+$ *m*/*z* = 387.0 $[M - H]^-$. HPLC: t_R = 5.70 min (100.0 % purity).

*4.2.5.47. 2-Methyl-1-((2-(trimethylsilyl)ethoxy)methyl)-1H-imidazole (**22**)*

2-Methylimidazole (**21**) (925 mg, 11.27 mmol) was dissolved in THF (40 mL), cooled to 0 °C and sodium hydride 60 % in mineral oil (500 mg, 12.50 mmol) was added portionwise over 5 min. After 30 min of stirring at 0 °C, 2-(trimethylsilyl)ethoxymethyl chloride (2.00 mL, 11.30 mmol) was added dropwise and the mixture was stirred at rt for 18 h. Purification by flash chromatography (SiO_2, *n*-hexane/EtOAc 90:10 to 60:40) afforded **22** as a clear oil (2.30 g, 96 %). ^{1}H NMR (300 MHz, $CDCl_3$) δ -0.02 (s, 9H), 0.82 - 0.95 (m, 2H), 2.43 (s, 3H), 3.39 - 3.53 (m, 2H), 5.18 (s, 2H), 6.90 (s, 2H).

*4.2.5.48. 2-Methyl-5-(tributylstannyl)-1-((2-(trimethylsilyl)ethoxy)methyl)-1H-imidazole (**23**)*

The title compound was synthesized according to a previously reported method[34] to give **23** as a clear oil (1.41 g, 25 %). ^{1}H NMR (300 MHz, $CDCl_3$) δ 0.00 (s, 9H), 0.85 - 0.96 (m, 12H), 1.02 - 1.11 (m, 5H), 1.25 - 1.40 (m, 7H), 1.46 - 1.56 (m, 5H), 2.48 (s, 3H), 3.37 - 3.47 (m, 2H), 5.14 (s, 2H), 6.90 (s, 1H). TLC-MS (ESI) *m*/*z* = 373.0 $[M + H]^+$.

*4.2.5.49. N-(4-(2-Methyl-1-((2-(trimethylsilyl)ethoxy)methyl)-1H-imidazol-5-yl)pyridin-2-yl)cyclopropanecarboxamide (**24**)*

Compound **23** (462 mg, 0.92 mmol), *N*-(4-bromopyridin-2-yl)cyclopropanecarboxamide (222 mg, 0.92 mmol) and $Pd(PPh_3)_4$ (77 mg, 0.069 mmol) were dissolved in degassed 1,4-dioxane (9 mL) under an atmosphere of argon. The reaction mixture was heated to 105 °C for 18 h before the solution was filtered through a pad of Celite. The pad was washed with DCM (30 mL) and the solvents were removed under reduced pressure. Purification by flash chromatography (SiO_2, DCM/EtOH 95:05) afforded **24** as an off-white solid (265 mg, 77 %). ^{1}H NMR (300 MHz, $CDCl_3$) δ -0.04 (s, 9H), 0.84 - 0.92 (m, 4H), 1.06 - 1.15 (m, 2H), 1.55 - 1.67 (m, 1H), 2.53 (s, 3H), 3.45 - 3.55 (m, 2H), 5.28 (s, 2H), 7.16 (dd, *J* = 5.3, 1.6 Hz, 1H), 7.18 (s, 1H), 8.27 (dd, *J* = 5.2, 0.6 Hz, 1H), 8.30 (d, *J* = 0.6 Hz, 1H), 9.17 (s, 1H).

^{13}C NMR (75 MHz, $CDCl_3$) δ -1.5, 8.3, 13.7, 15.7, 17.7, 66.0, 72.7, 112.2, 118.0, 128.6, 131.3, 140.0, 148.0, 148.8, 152.2, 172.5. TLC-MS (ESI) *m*/*z* = 394.9 $[M + Na]^+$ *m*/*z* = 371.0 $[M - H]^-$. HPLC: t_R = 5.99 min (100.0 % purity).

*4.2.5.50. N-(4-(2-Methyl-1H-imidazol-5-yl)pyridin-2-yl)cyclopropanecarboxamide (**25**)*

Compound **24** (69 mg, 0.19 mmol) was dissolved in DCM (2 mL) before TFA (2 mL) was added and the solution was stirred for 6 h at rt. Sat. sodium bicarbonate solution (15 mL) was added and the organic layer was separated. The aqueous phase was extracted with DCM (4x) and the combined organic layers were dried over anhydrous Na_2SO_4 before the solvent was removed under reduced pressure. Purification by flash chromatography (SiO_2, DCM/EtOH 95:05 to 90:10) afforded **25** as a tan white solid (40 mg, 89 %). ^{1}H NMR (300 MHz, DMSO-d_6) δ 0.74 - 0.86 (m, 4H), 1.96 - 2.06 (m, 1H), 2.32 (s, 3H), 7.35 (dd, *J* = 5.2, 1.6 Hz, 1H), 7.61 (s, 1H), 8.18 (d, *J* = 5.2 Hz, 1H), 8.40 (d, *J* = 0.4 Hz, 1H), 10.64 (s, 1H), 12.07 (br. s., 1H). ^{13}C NMR (75 MHz, DMSO-d_6) δ 7.6, 13.8, 14.3, 108.1, 114.5, 116.6, 136.5, 143.5, 145.4, 147.9, 152.7, 172.5. TLC-MS (ESI) *m*/*z* = 243.0 $[M + H]^+$ *m*/*z* = 241.0 $[M - H]^-$. HPLC: t_R = 1.35 min (99.1 % purity).

*4.2.5.51. N-(Cyclopropylmethyl)-4-(4-(4-fluorophenyl)-2-(methylthio)-1H-imidazol-5-yl)pyridin-2-amine (**26**)*

Compound **11a** (100 mg, 0.31 mmol) and cyclopropanemethylamine (545 µL, 6.29 mmol were combined in a small reaction vessel. The reaction was heated to 160 °C for 48 h. The reaction mixture was allowed to cool to rt and H_2O (15 mL) was added. It was extracted with ethyl acetate (3x) and the combined organic layers were washed with brine. After drying over anhydrous Na_2SO_4 the solvent was removed under reduced pressure and purified by flash chromatography (SiO_2, DCM/EtOH 97:03) afforded **26** as a yellow solid (23 mg, 21 %). ^{1}H NMR (300 MHz, MeOD) δ 0.15 - 0.22 (m, 2H), 0.43 - 0.52 (m, 2H), 0.91 - 1.08 (m, 1H), 2.61 (s, 3H), 3.02 (d, *J* = 6.8 Hz, 2H), 6.52 (dd, *J* = 5.5, 1.4 Hz, 1H), 6.57 (s, 1H), 7.05 - 7.17 (m, 2H), 7.38 - 7.49 (m, 2H), 7.79 (dd, *J* = 5.5, 0.4 Hz, 1H). ^{13}C NMR

(75 MHz, MeOD) δ 4.0, 11.7, 17.0, 47.8, 107.0, 111.8, 116.7 (d, $^{2}J_{CF}$ = 21.6 Hz), 131.8 (d, $^{3}J_{CF}$ = 8.3 Hz), 144.6, 148.3, 160.7, 164.1 (d, $^{1}J_{CF}$ = 246.6 Hz). TLC-MS (ESI) *m*/*z* = 355.5 $[M + H]^+$ *m*/*z* = 353.4 $[M - H]^-$. HPLC: t_R = 5.08 min (100.0 % purity).

4.3. GSK3 assay

Inhibitory activity on GSK3α and β was evaluated by using the ADP-Glo™ Kinase Assay kit from Promega (Promega Corporation, Madison, WI 53711, USA).[36] The assay was performed in white, non-treated 384-well plates (Corning) using a concentration of 0.50 ng/μL of recombinant human GSK3α or 0.58 ng/μL of recombinant human GSK3β, 25 μM ATP, and 0.2 μg/μL GSK3 substrate G50-58 (sequence: YRRAAVPPSPSLSRHSSPHQ(pS)EDEEE) in presence of serial dilutions of test compounds. A control consisting of uninhibited kinase and one presenting ATP/substrate solution were also included in the plate. Kinase was pre-incubated with the test compounds for 10 min at rt and the reaction was then started with the addition of substrate/ATP and run for 60 min at rt. After the addition of ADP-Glo™ reagent (5 μL, 60 min incubation) and Kinase detection reagent (10 μL, 30 min incubation), the luminescence was measured using a FilterMax F5 microplate reader (Molecular Devices) with an integration time of 500 ms. Raw data were normalized to the values of control wells and analyzed using the software GraphPad Prism v.7.03. Each experiment was performed two times in quadruplicate.

4.4. Molecular Modeling

All the modeling was conducted with Maestro Small-Molecule Drug Discovery Suite 2017-4 (Schrödinger, LLC) with OPLS3 force field.[52] Prior to docking, the small-molecules were prepared with LipPrep (default settings) using Epik[53, 54] to generate the potential

tautomers and ionization states. The Induced Fit docking[39-41] was performed with the GSK3β crystal structure (PDB ID: 4PTC), which was prepared using Protein Preparation Wizard (default settings).[55] The box center was defined by the co-crystalized ligand. H-bond constrains were applied to the hinge region Val 135 (backbone NH and O). The default settings were used in the IFD, except the Glide redocking was conducted with XP precision.[56] The MD simulation was conducted with Desmond.[57] The system was solvated in a cubic box (edges 13Å from the protein) and neutralized with counterions (Cl^-). The water was described with TIP3P water model.[58] The final system consisted of 58,185 atoms. The default relaxation protocol was used before the 200ns production simulation, which was conducted in NPT ensemble (300 K; 1.01325 bar). The figures were prepared with PyMOL 2.2.3 (Schrödinger, LLC).

Acknowledgments

We thank Jens Strobach and Katharina Bauer for their assistance in the p38α MAP kinase ELISA activity assay. We appreciate the helpful comments of Johannes Heidrich on the use of PyMOL and Schrödinger Maestro. This study was supported by the Federal Ministry of Education and Research (BMBF) within the BioPharma-Neuroallianz consortium (Neuro-T8B project).

Appendix A. Supplementary data

Supplementary data to this article can be found online at https://doi.org/j.ejmech.XXXX.XXXXX.

Abbreviations

AD	Alzheimer's disease;
GSK3	glycogen synthase kinase 3

MAP	mitogen-activated protein
PyBOP	(benzotriazol-1-yloxy)tripyrrolidinophosphonium hexafluorophosphate
HATU	1-[bis(dimethylamino)methylene]-1*H*-1,2,3-triazolo[4,5-*b*]pyridinium 3-oxide hexafluorophosphate
HWB	human whole blood
LPS	lipopolysaccharide
NaHMDS	sodium hexamethyldisilazide
SEM	2-(trimethylsilyl)ethoxymethyl
TFA	trifluoroacetic acid
TNF-α	tumor necrosis factor-α.

Notes

The authors declare no competing financial interest.

References

[1] M.C.-H. Prince, A.; Knapp, M.; Guerchet, M.; Karagiannidou, M., World Alzheimer report 2016: improving healthcare for people living with dementia: coverage, quality and costs now and in the future., Alzheimer's Disease International (ADI), London, UK., (2016).

[2] C. Hooper, R. Killick, S. Lovestone, The GSK3 hypothesis of Alzheimer's disease, J. Neurochem., 104 (2008) 1433–1439.

[3] A. Kremer, J.V. Louis, T. Jaworski, F. van Leuven, GSK3 and Alzheimer's Disease: Facts and Fiction, Front. Mol. Neurosci., 4 (2011) 17.

[4] M. Llorens-Martin, J. Jurado, F. Hernandez, J. Avila, GSK-3beta, a pivotal kinase in Alzheimer disease, Front. Mol. Neurosci., 7 (2014) 46.

[5] A. Takashima, GSK-3 is essential in the pathogenesis of Alzheimer's disease, J. Alzheimer's Dis., 9 (2006) 309–317.

[6] A. Cavallini, S. Brewerton, A. Bell, S. Sargent, S. Glover, C. Hardy, R. Moore, J. Calley, D. Ramachandran, M. Poidinger, E. Karran, P. Davies, M. Hutton, P. Szekeres, S. Bose, An unbiased approach to identifying tau kinases that phosphorylate tau at sites associated with Alzheimer disease, J. Biol. Chem., 288 (2013) 23331–23347.

[7] J.-Z. Wang, I. Grundke-Iqbal, K. Iqbal, Kinases and phosphatases and tau sites involved in Alzheimer neurofibrillary degeneration, Eur. J. Neurosci., 25 (2007) 59–68.

[8] B. DaRocha-Souto, M. Coma, B.G. Perez-Nievas, T.C. Scotton, M. Siao, P. Sanchez-Ferrer, T. Hashimoto, Z. Fan, E. Hudry, I. Barroeta, L. Sereno, M. Rodriguez, M.B. Sanchez, B.T. Hyman, T. Gomez-Isla, Activation of glycogen synthase kinase-3 beta mediates beta-amyloid induced neuritic damage in Alzheimer's disease, Neurobiol. Dis., 45 (2012) 425-437.

[9] P.T. Ly, Y. Wu, H. Zou, R. Wang, W. Zhou, A. Kinoshita, M. Zhang, Y. Yang, F. Cai, J. Woodgett, W. Song, Inhibition of GSK3beta-mediated BACE1 expression reduces Alzheimer-associated phenotypes, J. Clin. Invest., 123 (2013) 224-235.

[10] A.K. Rana, D. Singh, Targeting glycogen synthase kinase-3 for oxidative stress and neuroinflammation: Opportunities, challenges and future directions for cerebral stroke management, Neuropharmacology, 139 (2018) 124-136.

[11] R.G. Canter, J. Penney, L.-H. Tsai, The road to restoring neural circuits for the treatment of Alzheimer's disease, Nature, 539 (2016) 187–196.

[12] E. Herlaar, Z. Brown, p38 MAPK signalling cascades in inflammatory disease, Mol. Med. Today, 5 (1999) 439–447.

[13] J.C. Lee, J.T. Laydon, P.C. McDonnell, T.F. Gallagher, S. Kumar, D. Green, D. McNulty, M.J. Blumenthal, J.R. Heys, S.W. Landvatter, A protein kinase involved in the regulation of inflammatory cytokine biosynthesis, Nature, 372 (1994) 739–746.

[14] K. Hensley, R.A. Floyd, N.-Y. Zheng, R. Nael, K.A. Robinson, X. Nguyen, Q.N. Pye, C.A. Stewart, J. Geddes, W.R. Markesbery, E. Patel, G.V.W. Johnson, G. Bing, p38 Kinase Is Activated in the Alzheimer's Disease Brain, J. Neurochem., 72 (1999) 2053–2058.

[15] A.D. Bachstetter, B. Xing, L. Almeida, E.R. Dimayuga, D.M. Watterson, L.J. van Eldik, Microglial p38alpha MAPK is a key regulator of proinflammatory cytokine up-regulation induced by toll-like receptor (TLR) ligands or beta-amyloid (Abeta), J. Neuroinflammation, 8 (2011) 79.

[16] L. Munoz, A.J. Ammit, Targeting p38 MAPK pathway for the treatment of Alzheimer's disease, Neuropharmacology, 58 (2010) 561–568.

[17] L. Munoz, H. Ralay Ranaivo, S.M. Roy, W. Hu, J.M. Craft, L.K. McNamara, L.W. Chico, L.J. van Eldik, D.M. Watterson, A novel p38 alpha MAPK inhibitor suppresses brain proinflammatory cytokine up-regulation and attenuates synaptic dysfunction and behavioral deficits in an Alzheimer's disease mouse model, J. Neuroinflammation, 4 (2007) 21.

[18] A. Sun, M. Liu, X.V. Nguyen, G. Bing, P38 MAP kinase is activated at early stages in Alzheimer's disease brain, Exp. Neurol., 183 (2003) 394–405.

[19] N. Maphis, S. Jiang, G. Xu, O.N. Kokiko-Cochran, S.M. Roy, L.J. Van Eldik, D.M. Watterson, B.T. Lamb, K. Bhaskar, Selective suppression of the alpha isoform of p38 MAPK rescues late-stage tau pathology, Alzheimer's Res. Ther., 8 (2016) 54.

[20] J. Alam, K. Blackburn, D. Patrick, Neflamapimod: Clinical Phase 2b-Ready Oral Small Molecule Inhibitor of p38alpha to Reverse Synaptic Dysfunction in Early Alzheimer's Disease, J. Prev. Alzheimer's Dis., 4 (2017) 273-278.

[21] P. Scheltens, N. Prins, A. Lammertsma, M. Yaqub, A. Gouw, A.M. Wink, H.M. Chu, B.N.M. van Berckel, J. Alam, An exploratory clinical study of p38alpha kinase inhibition in Alzheimer's disease, Ann. Clin. Transl. Neurol., 5 (2018) 464-473.

1402 [22] F. Ansideri, S. Andreev, A. Kuhn, W. Albrecht, S. Laufer, P. Koch, A Diverse and
1403 Versatile Regiospecific Synthesis of Tetrasubstituted Alkylsulfanylimidazoles as p38α
1404 Mitogen-Activated Protein Kinase Inhibitors, Molecules, 23 (2018) 221.
1405 [23] A. Cuenda, J. Rouse, Y.N. Doza, R. Meier, P. Cohen, T.F. Gallagher, P.R. Young,
1406 J.C. Lee, SB 203580 is a specific inhibitor of a MAP kinase homologue which is stimulated
1407 by cellular stresses and interleukin-1, FEBS Lett., 364 (1995) 229–233.
1408 [24] P. Koch, C. Bäuerlein, H. Jank, S. Laufer, Targeting the ribose and phosphate binding
1409 site of p38 mitogen-activated protein (MAP) kinase: Synthesis and biological testing of 2-
1410 alkylsulfanyl-, 4(5)-aryl-, 5(4)-heteroaryl-substituted imidazoles, J. Med. Chem., 51 (2008)
1411 5630-5640.
1412 [25] S. Laufer, D. Hauser, T. Stegmiller, C. Bracht, K. Ruff, V. Schattel, W. Albrecht, P.
1413 Koch, Tri- and tetrasubstituted imidazoles as p38alpha mitogen-activated protein kinase
1414 inhibitors, Bioorg. Med. Chem. Lett., 20 (2010) 6671–6675.
1415 [26] S.A. Laufer, G.K. Wagner, D.A. Kotschenreuther, W. Albrecht, Novel substituted
1416 pyridinyl imidazoles as potent anticytokine agents with low activity against hepatic
1417 cytochrome P450 enzymes, J. Med. Chem., 46 (2003) 3230-3244.
1418 [27] J. Halekotte, L. Witt, C. Ianes, M. Kruger, M. Buhrmann, D. Rauh, C. Pichlo, E.
1419 Brunstein, A. Luxenburger, U. Baumann, U. Knippschild, J. Bischof, C. Peifer, Optimized
1420 4,5-Diarylimidazoles as Potent/Selective Inhibitors of Protein Kinase CK1delta and Their
1421 Structural Relation to p38alpha MAPK, Molecules, 22 (2017) 522.
1422 [28] M. Semones, Y. Feng, N. Johnson, J.L. Adams, J. Winkler, M. Hansbury,
1423 Pyridinylimidazole inhibitors of Tie2 kinase, Bioorg. Med. Chem. Lett., 17 (2007) 4756–
1424 4760.
1425 [29] F. Muth, A. El-Gokha, F. Ansideri, M. Eitel, E. Döring, A. Sievers-Engler, A. Lange,
1426 F.M. Boeckler, M. Lämmerhofer, P. Koch, S.A. Laufer, Tri- and Tetrasubstituted

1427 Pyridinylimidazoles as Covalent Inhibitors of c-Jun N-Terminal Kinase 3, J. Med. Chem.,
1428 60 (2017) 594-607.
1429 [30] F. Muth, M. Günther, S.M. Bauer, E. Döring, S. Fischer, J. Maier, P. Drückes, J.
1430 Köppler, J. Trappe, U. Rothbauer, P. Koch, S.A. Laufer, Tetra-Substituted
1431 Pyridinylimidazoles As Dual Inhibitors of p38 alpha Mitogen-Activated Protein Kinase and
1432 c-Jun N-Terminal Kinase 3 for Potential Treatment of Neurodegenerative Diseases (vol 58,
1433 pg 443, 2015), J. Med. Chem., 58 (2015) 2567-2567.
1434 [31] P. Koch, F. Ansideri, 2-Alkylsulfanyl-4(5)-aryl-5(4)-heteroarylimidazoles: An Overview
1435 on Synthetic Strategies and Biological Activity, Arch. Pharm., 350 (2017) e1700258.
1436 [32] S.A. Laufer, A.J. Liedtke, A concise and optimized four-step approach toward 2-(aryl-
1437)alkylsulfanyl-, 4(5)-aryl-, 5(4)-heteroaryl-substituted imidazoles using alkyl- or arylalkyl
1438 thiocyanates, Tetrahedron Lett., 47 (2006) 7199-7203.
1439 [33] F. Heider, U. Haun, E. Döring, M. Kudolo, C. Sessler, W. Albrecht, S. Laufer, P. Koch,
1440 From 2-alkylsulfanylimidazoles to 2-alkylimidazoles: An approach towards metabolically
1441 more stable p38α MAP kinase inhibitors, Molecules, 22 (2017) 1729.
1442 [34] M.D. Markey, T.R. Kelly, Synthesis of cribrostatin 6, J. Org. Chem., 73 (2008) 7441-
1443 7443.
1444 [35] M. Goettert, R. Graeser, S.A. Laufer, Optimization of a nonradioactive immunosorbent
1445 assay for p38alpha mitogen-activated protein kinase activity, Anal. Biochem., 406 (2010)
1446 233–234.
1447 [36] H. Zegzouti, M. Zdanovskaia, K. Hsiao, S.A. Goueli, ADP-Glo: A Bioluminescent and
1448 homogeneous ADP monitoring assay for kinases, Assay Drug Dev. Technol., 7 (2009)
1449 560–572.
1450 [37] S.M. Bauer, J.M. Kubiak, U. Rothbauer, S. Laufer, From Enzyme to Whole Blood:
1451 Sequential Screening Procedure for Identification and Evaluation of p38 MAPK Inhibitors,

in: H. Zegzouti, S. Goueli (Eds.) Kinase Screening and Profiling, Humana Press New York, NY, 2016, pp. 123-148.

[38] S. Blencke, B. Zech, O. Engkvist, Z. Greff, L. Orfi, Z. Horváth, G. Kéri, A. Ullrich, H. Daub, Characterization of a conserved structural determinant controlling protein kinase sensitivity to selective inhibitors, Chem. Biol., 11 (2004) 691–701.

[39] R. Farid, T. Day, R.A. Friesner, R.A. Pearlstein, New insights about HERG blockade obtained from protein modeling, potential energy mapping, and docking studies, Bioorg. Med. Chem., 14 (2006) 3160-3173.

[40] W. Sherman, T. Day, M.P. Jacobson, R.A. Friesner, R. Farid, Novel procedure for modeling ligand/receptor induced fit effects, J. Med. Chem., 49 (2006) 534-553.

[41] W. Sherman, H.S. Beard, R. Farid, Use of an induced fit receptor structure in virtual screening, Chem. Biol. Drug Des., 67 (2006) 83-84.

[42] F. Ansideri, J.T. Macedo, M. Eitel, A. El-Gokha, D.S. Zinad, C. Scarpellini, M. Kudolo, D. Schollmeyer, F.M. Boeckler, B.S. Blaum, S.A. Laufer, P. Koch, Structural optimization of a pyridinylimidazole scaffold: shifting the selectivity from p38α mitogen-activated protein kinase to c-Jun N-terminal kinase 3., ACS Omega, 3 (2018) 7809-7831.

[43] C.E. Fitzgerald, S.B. Patel, J.W. Becker, P.M. Cameron, D. Zaller, V.B. Pikounis, S.J. O'Keefe, G. Scapin, Structural basis for p38 alpha MAP kinase quinazolinone and pyridol-pyrimidine inhibitor specificity, Nat. Struct. Biol., 10 (2003) 764-769.

[44] H. Pajouhesh, G.R. Lenz, Medicinal chemical properties of successful central nervous system drugs, NeuroRx, 2 (2005) 541-553.

[45] S.G. Krimmer, J. Cramer, M. Betz, V. Fridh, R. Karlsson, A. Heine, G. Klebe, Rational Design of Thermodynamic and Kinetic Binding Profiles by Optimizing Surface Water Networks Coating Protein-Bound Ligands, J. Med. Chem., 59 (2016) 10530-10548.

[46] B. Kammerer, H. Scheible, G. Zurek, M. Godejohann, K.P. Zeller, C.H. Gleiter, W. Albrecht, S. Laufer, In vitro metabolite identification of ML3403, a 4-pyridinylimidazole-type

1478 p38 MAP kinase inhibitor by LC-Qq-TOF-MS and LC-SPE-cryo-NMR/MS, Xenobiotica, 37
1479 (2007) 280-297.
1480 [47] J.R. Woodgett, Molecular cloning and expression of glycogen synthase kinase-
1481 3/factor A, EMBO J., 9 (1990) 2431–2438.
1482 [48] F.F. Wagner, L. Benajiba, A.J. Campbell, M. Weiwer, J.R. Sacher, J.P. Gale, L. Ross,
1483 A. Puissant, G. Alexe, A. Conway, M. Back, Y. Pikman, I. Galinsky, D.J. DeAngelo, R.M.
1484 Stone, T. Kaya, X. Shi, M.B. Robers, T. Machleidt, J. Wilkinson, O. Hermine, A. Kung, A.J.
1485 Stein, D. Lakshminarasimhan, M.T. Hemann, E. Scolnick, Y.L. Zhang, J.Q. Pan, K.
1486 Stegmaier, E.B. Holson, Exploiting an Asp-Glu "switch" in glycogen synthase kinase 3 to
1487 design paralog-selective inhibitors for use in acute myeloid leukemia, Sci. Transl. Med., 10
1488 (2018) eaam8460.
1489 [49] F. Heider, U. Haun, E. Döring, M. Kudolo, C. Sessler, W. Albrecht, S. Laufer, P. Koch,
1490 From 2-Alkylsulfanylimidazoles to 2-Alkylimidazoles: An Approach towards Metabolically
1491 More Stable p38α MAP Kinase Inhibitors, Molecules, 22 (2017).
1492 [50] S. Bühler, M. Goettert, D. Schollmeyer, W. Albrecht, S.A. Laufer, Chiral Sulfoxides as
1493 Metabolites of 2-Thioimidazole-Based p38 alpha Mitogen-Activated Protein Kinase
1494 Inhibitors: Enantioselective Synthesis and Biological Evaluation, J. Med. Chem., 54 (2011)
1495 3283-3297.
1496 [51] S.J. Cho, N.H. Jensen, T. Kurome, S. Kadari, M.L. Manzano, J.E. Malberg, B.
1497 Caldarone, B.L. Roth, A.P. Kozikowski, Selective 5-hydroxytryptamine 2C receptor
1498 agonists derived from the lead compound tranylcypromine: Identification of drugs with
1499 antidepressant-like action, J. Med. Chem., 52 (2009) 1885–1902.
1500 [52] E. Harder, W. Damm, J. Maple, C. Wu, M. Reboul, J.Y. Xiang, L. Wang, D. Lupyan,
1501 M.K. Dahlgren, J.L. Knight, J.W. Kaus, D.S. Cerutti, G. Krilov, W.L. Jorgensen, R. Abel,
1502 R.A. Friesner, OPLS3: A Force Field Providing Broad Coverage of Drug-like Small
1503 Molecules and Proteins, J. Chem. Theory Comput., 12 (2016) 281-296.

[53] J.R. Greenwood, D. Calkins, A.P. Sullivan, J.C. Shelley, Towards the comprehensive, rapid, and accurate prediction of the favorable tautomeric states of drug-like molecules in aqueous solution, J. Comput.-Aided Mol. Des., 24 (2010) 591-604.

[54] J.C. Shelley, A. Cholleti, L.L. Frye, J.R. Greenwood, M.R. Timlin, M. Uchimaya, Epik: a software program for pK(a) prediction and protonation state generation for drug-like molecules, J. Comput.-Aided Mol. Des., 21 (2007) 681-691.

[55] G.M. Sastry, M. Adzhigirey, T. Day, R. Annabhimoju, W. Sherman, Protein and ligand preparation: parameters, protocols, and influence on virtual screening enrichments, J. Comput.-Aided Mol. Des., 27 (2013) 221-234.

[56] R.A. Friesner, R.B. Murphy, M.P. Repasky, L.L. Frye, J.R. Greenwood, T.A. Halgren, P.C. Sanschagrin, D.T. Mainz, Extra precision glide: docking and scoring incorporating a model of hydrophobic enclosure for protein-ligand complexes, J. Med. Chem., 49 (2006) 6177-6196.

[57] K.J. Bowers, C. Edmond, H. Xu, R.O. Dror, M.P. Eastwood, B.A. Gregerson, J.L. Klepeis, I. Kolossvary, M.A. Moraes, F.D. Sacerdoti, J.K. Salmon, Y. Shan, D.E. Shaw, Scalable Algorithms for Molecular Dynamics Simulations on Commodity Clusters, Proceedings of the ACM/IEEE Conference on Supercomputing (SC06), Tampa, Florida, November 11-17 (2006).

[58] W.L. Jorgensen, J. Chandrasekhar, J.D. Madura, R.W. Impey, M.L. Klein, Comparison of Simple Potential Functions for Simulating Liquid Water, J Chem Phys, 79 (1983) 926-935.

Highlights

- A series of 39 novel pyridinylimidazoles as dual inhibitors of synthase kinase 3β and p38α mitogen-activated protein kinase was designed and synthesized.
- The binding mode of these inhibitors is suggested by computational docking studies as well as by molecular dynamic simulations.
- Imidazole tautomerism may influence the interactions in the ATP binding site.
- Most promising dual inhibitor is metabolically stable and penetrates into the brain.